Coulomb effects in nuclear reactions with charged particles

L. D. Blokhintsev, A. M. Mukhamedzhanov, and A. N. Safronov

Scientific-Research Institute of Nuclear Physics, Moscow State University

Fiz. Elem. Chastits At. Yadra **15**, 1296–1337 (November–December 1984)

Coulomb effects in the amplitudes of nuclear processes are considered. An equation is derived for the Coulomb–nuclear vertex function, and also spectral and N/D representations for the Coulomb–nuclear amplitude. The K-matrix formalism is generalized to the case of Coulomb–nuclear scattering. Charged-particle stripping reactions to resonance states are analyzed theoretically. A study is made of the analytic properties of the nonrelativistic Feynman diagrams in the presence of a Coulomb interaction, and it is shown that the Coulomb effects lead to the appearance of a pole singularity in nonpole diagrams (triangle diagram, etc.). The methods considered can be used to describe concrete nuclear reactions with the participation of charged particles; varied spectroscopic information is extracted.

INTRODUCTION

It is well known that the addition of the long-range Coulomb interaction to the short-range nuclear potential leads to a significant change in the behavior of the wave functions of the scattering problem at large distances and, as a consequence, to a different energy dependence of the scattering amplitudes at low energies. These specific features of the Coulomb interaction, which are important for a number of practical applications, in particular the problem of controlled thermonuclear fusion, are clearly manifested already in the simplest case of the two-body potential problem. For a large number of bodies, allowance for the Coulomb interaction complicates the already difficult problem of solving the corresponding equations.

In the theory of systems of particles with a strong interaction, which includes the theory of nuclear reactions, wide use has been made in recent years of different diagrammatic and dispersion methods (see, for example, Refs. 1–3). For the use of these methods, the analytic properties of the scattering amplitudes are of the first importance. However, the Coulomb interaction radically changes the analytic properties of not only the complete amplitude but also the individual diagrams, so that the approaches developed for short-ranges potentials become invalid. It is necessary to separate correctly the specific "Coulomb" singularities of the scattering amplitudes.

This review investigates the influence of Coulomb effects on the properties (in the first place, the analytic properties) of the scattering amplitudes and the modifications to the various approaches in the theory of nuclear reactions made necessary by the Coulomb interaction.

In Sec. 1 we briefly discuss the analytic structure of the potential Coulomb–nuclear amplitude on the energy shell.

In Secs. 2 and 3 we derive equations for the off-shell Coulomb–nuclear amplitude and for the Coulomb–nuclear vertex function, and also spectral and N/D representations for the Coulomb–nuclear amplitude.

Section 4 generalizes the K-matrix formalism to Coulomb–nuclear scattering.

In Sec. 5 we discuss a method for calculating Coulomb–nuclear interference effects on the basis of the N/D equations.

The methods considered in Secs. 1–5 are used in Sec. 6 to analyze quantitatively various nuclear processes and to extract spectroscopic information from experimental data.

Section 7 is devoted to the theoretical analysis of charged-particle stripping reactions to resonance states.

In Sec. 8 we investigate the analytic properties of nonrelativistic Feynman diagrams in the presence of the Coulomb interaction.

Finally, in Sec. 9 we consider in detail in the framework of a model of three charged particles the Coulomb effects in nucleon or cluster transfer reactions.

1. ANALYTIC STRUCTURE OF THE PARTIAL-WAVE ON-SHELL COULOMB-NUCLEAR AMPLITUDE

We consider the problem of nonrelativistic potential scattering of two spinless particles whose interaction is the sum of a Coulomb and a short-range potential. Suppose that the short-range potential $V_n(r)$ is a superposition of Yukawa potentials,

$$V_n(r) = \int_{\varkappa_0}^{\infty} \sigma(\varkappa) \frac{e^{-\varkappa r}}{r} d\varkappa, \tag{1}$$

and that the Coulomb potential is repulsive. The analytic properties of the partial-wave scattering amplitudes on the energy shell for this case were investigated in Refs. 4–8. The main result of these investigations is that the reduced partial-wave amplitude $A_l(s)$ ($s = k^2$, where k is the relative momentum of the colliding particles), which is related to the partial-wave S matrix by

$$S_l = 1 + 2i\,\rho_l(s)\,A_l(s), \tag{2}$$

where $\rho_l(s) = s^{l+1/2}$, can be represented in the form

$$A_l(s) = A_l^{(c)}(s) + [h_l^{(c)}(\sqrt{s})]^{-2} T_l(s). \tag{3}$$

Here,

$$h_l^{(c)}(k) = \frac{l!\exp\left(\frac{\pi}{2}\eta\ \mathrm{sign}\,\mathrm{Re}\,k\right)}{\Gamma(l+1+i\eta)} \tag{4}$$

is the normalized ($h_l^{(c)}(k) \underset{k\to\infty}{\to} 1$) Coulomb Jost function; $A_l^{(c)}(s)$ is the reduced partial-wave amplitude of the scattering by the Coulomb potential; $\eta = \lambda/k$ is the Coulomb Sommerfeld parameter, $\lambda = \mu\alpha Z_1 Z_2 > 0$; μ is the reduced mass of the

 0090-4759/84/060580-20$04.40

particles; Z_1 and Z_2 are their charges; and α is the fine-structure constant. The amplitude $T_l(s)$ is the renormalized Coulomb–nuclear scattering amplitude. On the first (physical) sheet of the Riemann surface of the complex variable s, $T_l(s)$ has the same analytic structure as the amplitude of scattering by a short-range potential, namely, it has a left-hand (dynamical) cut C_L and a right-hand (unitarity) cut C_R, the discontinuity across it being determined by the expression

$$\operatorname{Im} T_l(s) = \theta(s)\,\tilde{\rho}_l(s)\,|T_l(s)|^2, \tag{5}$$

where $\theta(x) = 1$ (0) for $x > 0$ ($x < 0$), and[1)]

$$\tilde{\rho}_l(s) = \rho_l(s)\,C_l^2(s),\quad C_l^2(s) \equiv \left|h_l^{(c)}(\sqrt{s})\right|^{-2} = \frac{\pi\eta}{\operatorname{sh}(\pi\eta)}\,e^{-\pi\eta}\prod_{m=1}^{l}(1+\eta^2/m^2). \tag{6}$$

It follows from these properties that the renormalized amplitude $T_l(s)$ is analogous to the reduced partial-wave amplitude for scattering by a short-range potential. However, there is a difference between the analytic properties of these amplitudes on the other sheets of the Riemann surface and in the neighborhood of the point $s = 0$. On the second sheet in the plane of the variable $k = \sqrt{sT}_l(s)$ there is a cut $-i\infty < k \leqslant 0$; at the points $k = i\lambda/(n+l)$ $(n = 1,2,\ldots)$ there is an infinite sequence of zeros, and at points nearby there is an infinite sequence of poles, the point $s = 0$ being an accumulation point of the poles. Nevertheless, on the physical sheet the amplitude $T_l(s)$ is bounded in the neighborhood of the point $s = 0$ and as $s \to 0$ behaves as follows:

$$T_l(s) \underset{s\to 0}{\cong} \left\{R_l(s) - 2\pi i\,\frac{\lambda^{2l+1}}{(l!)^2}\,e^{-\frac{2\pi\lambda}{\sqrt{s}}}\right\}, \tag{7}$$

where $R_l(s)$ is a function regular in the neighborhood of $s = 0$. One can show (see below) that the amplitude $T_l(s)$ satisfies the N/D representation $T_l(s) = N_l(s)/D_l(s)$, where $N_l(s)$ has only a left-hand cut, and $D_l(s)$ only a right-hand cut. These functions are the solutions of a system of nonsingular equations analogous to the usual N/D equations (see, for example, Ref. 9), with the only difference that instead of the spectral function $\rho_l(s)$ they contain the function $\tilde{\rho}_l(s)$ [see Eq. (6)], and the so-called potential function $L_l(s)$ is completely determined by the discontinuity of the renormalized amplitude across the left-hand cut (i.e., $\operatorname{Im} L_l(s) = \operatorname{Im} T_l(s)$ on C_L).[8]

If the system has a bound state, the amplitude $T_l(s)$ has a pole on the first sheet at $s = s_a$. The residue of $T_l(s)$ at this pole can be related to the vertex constant[2)] G_l of virtual disintegration of the bound state into two fragments, determined with allowance for the Coulomb interaction between the fragments[10]:

$$\lim_{s\to s_a}[(s-s_a)\,s^l T_l(s)] = -\frac{\mu^2}{\pi}\,\tilde{G}_l^2. \tag{8}$$

It can be shown that the constant $\tilde{G}_l^2$ defined in this manner is a real quantity (this result follows, for example, from the N/D equations). When the Coulomb interaction is eliminated, the definition (8) agrees with the definition of the vertex constant in the review of Ref. 2 for the case of a short-range interaction. Note that the constant $\tilde{G}_l$ is related to the vertex constant G_l defined in Ref. 2 (see Eq. (119) of that review) by

$$G_l = \exp\left(\frac{i\pi\eta_0}{2}\right)\frac{\Gamma(l+1+\eta_0)}{l!}\,\tilde{G}_l,$$

where $\eta_0 = \lambda/\varkappa$, $\varkappa = \sqrt{-s_a}$.

2. EQUATION FOR THE OFF-SHELL COULOMB–NUCLEAR AMPLITUDE AND *N/D* REPRESENTATION

The Coulomb–nuclear scattering problem can be solved in two equivalent ways. In the first, the integral equations of the scattering problem are formulated in terms of the matrix elements of the transition operator between Coulomb asymptotic state.[11] In the other approach, one takes a screened Coulomb potential V_c^R with sufficiently large screening radius in the Lippmann–Schwinger equation for the transition operator $t(s)$. In the case of a repulsive Coulomb interaction that we consider, the basic equation can be rearranged by going over to the Coulomb representation and renormalizing the matrix elements of the scattering operator. These renormalized matrix elements tend to a definite limit as $R \to \infty$ and satisfy an integral equation having a Fredholm operator as the kernel. Using the two-potential formula of Ref. 12 and making a partial-wave expansion, we obtain for the matrix elements of the Coulomb–nuclear part of the scattering operator $t_{cn}^R(s)$ the equation[8]

$$\begin{aligned}
t_l^{cn}(p',\ p;\ s) &= v_l^{(+)}(p',\ p) + \\
&+ \frac{2}{\pi}\int_0^\infty dp''\,\frac{p''^2}{p''^2 - s - i\varepsilon}\,v_l^{(-)}(p',\ p'')\,t_l^{(cn)}(p'',\ p;\ s),\\
v_l^{(\pm)}(p',\ p) &= -\frac{\mu}{2\pi}\langle p_c'^{(-)},\ l|V_n|p_c^{(\pm)},\ l\rangle,\\
t_l^{(cn)}(p', p;\ s) &= -\frac{\mu}{2\pi}\langle p_c'^{(-)},\ l|t_{cn}^R(s)|p_c^{(+)},\ l\rangle.
\end{aligned} \tag{9}$$

The Coulomb "in" and "out" partial-wave states $|p_c^{(\pm)}, l\rangle$ are normalized by

$$\langle p_c'^{(\pm)},\ l|p_c^{(\pm)},\ l\rangle = \frac{\pi}{2}\,\frac{1}{p^2}\,\delta(p-p'). \tag{10}$$

The matrix elements $v_l^{(\pm)}(p',p)$ and $t_l^{(cn)}(p',p;s)$ in the limit $R \to \infty$ contain Coulomb singularities with respect to the variables p and p', the sources of which are the "in" and "out" Coulomb wave functions. These singularities can be separated by going over from the matrix elements in terms of the "in" and "out" solutions to the matrix elements in terms of the regular solution of the Schrödinger equation with the boundary condition $\lim_{r\to 0} r^{-(l+1)}\varphi_l(p,r) = 1$. Since the boundary condition for $\varphi_l(p,r)$ does not depend on p, it follows from Poincaré's theorem[9] that this solution is an entire function of p. Using the relation

$$\langle r|p_c^{(\pm)},\ l\rangle = \frac{(ip)^l}{(2l+1)!!\,f_l^{(\pm)}(p)}\,\frac{\varphi_l(p,\ r)}{r}, \tag{11}$$

where $f_l^{(\pm)}(p)$ is the Jost function for the screened Coulomb

[1)] *Translator's Note.* The Russian notation for the trigonometric, inverse trigonometric, hyperbolic trigonometric functions, etc., is retained here and throughout the article in the displayed equations.

[2)] The expression "nuclear vertex constants" was used in the review of Ref. 2.

potential, we introduce the renormalized matrix elements of the operators V_n and t_{cn}^R by

$$v_l^{(\pm)}(p',\ p) = (p'p)^l\,[f_l^{*(-)}(p')\,f_l^{(\pm)}(p)]^{-1}w_l(p',\ p),$$
$$t_l^{(cn)}(p',\ p;\ s) = (p'p)^l\,[f_l^{*(-)}(p')\,f_l^{(+)}(p)]^{-1}\tau_l(p',\ p;\ s). \quad (12)$$

In the limit $R\to\infty$, the functions $f_l^{(+)}(p)$ and $f_l^{*(-)}(p)$ for real and positive p differ only by a phase factor of the form $\exp[\eta\ln(2pR)]$ from the normalized Coulomb Jost function $h_l^{(c)}(p)$ defined by Eq. (4), and the amplitude $\tau_l(p',p;s)$ for $p'=p=\sqrt{s}$ is equal to the renormalized one-shell amplitude $T_l(s)$ [see (3)]. The matrix elements of $w_l(p',p)$ have the same radius of analyticity with respect to the variables p and p' as the matrix elements of the short-range potential V_n. With allowance for (6), (9), and (12), the equation for the amplitude $\tau_l(p',p;s)$ in the limit $R\to\infty$ has the form

$$\tau_l(p',\ p;\ s) = w_l(p',\ p) + \frac{1}{\pi}\int_0^\infty \frac{ds'\tilde{\rho}_l(s')}{s'-s}\,w_l(p',\ \sqrt{s'})\,\tau(\sqrt{s'},\ p;\ s), \quad (13)$$

where the function $\tilde{\rho}_l(s)$ is determined by the expression (6).

Using the Fredholm method,[9] one can prove the validity of the N/D representation for the amplitude $T_l(s)$. To prove the convergence of the Fredholm series, it is sufficient to show that the kernel of the integral equation (13) is compact in the Banach space C_1 of continuous bounded functions with continuous bounded derivatives. The difference betwen the Lippmann–Schwinger equations and (13) is in the presence of the factor $C_l^2(q^2)$ in the kernel of Eq. (13). However, on the contour of integration (if we stay within the first sheet, the contour of integration is not deformed and is the half-axis from 0 to ∞) this factor is a continuous bounded function with a bounded derivative. Thus, for the first sheet the proof of compactness given in Ref. 13 for the Lippmann–Schwinger equation can be directly generalized to Eq. (13). Note that if we eliminate the purely imaginary values of k with $\mathrm{Im}k<0$, then the proof of compactness can also be extended to the second sheet of the Riemann surface; this is important for the investigation of resonance states, which correspond to poles on the second sheet.

If the interaction is determined by a nonlocal energy-dependent single-term separable potential with a form factor $\chi^{(l)}(p,s)$ of Hulthén type (in this case, $\chi^{(l)}(p,s)\to\bar{\chi}^{(l)}(p,s)=[p^2+\beta^2(s)]^{-(l+1)}$ when the Coulomb interaction is switched off), then the function $N_l(s)$ has the form

$$N_l(s) = \xi_l(s)\,\bar{N}_l(s), \quad (14)$$

where $\bar{N}_l(s)$ is $N_l(s)$ without the Coulomb interaction, and the factor

$$\xi_l(s) = \exp\left\{\frac{4\lambda}{p}\,\mathrm{arctg}\left[\frac{p}{\beta(s)}\right]\right\} \quad (15)$$

takes into account the Coulomb renormalization of the dynamical cut.

3. SPECTRAL REPRESENTATION FOR THE RENORMALIZED COULOMB–NUCLEAR AMPLITUDE. EQUATION FOR THE VERTEX FUNCTION

The operator equation for $t_{cn}^R(s)$ can be represented in the form

$$t_{cn}^R(s) = V_n + V_nG^R(s)\,V_n, \quad (16)$$

where $G^R(s)=(s/2\mu-H^s)^{-1}$, and $H^R=H_0+V_n+V_c^R$. Suppose the vectors $|\alpha,l\rangle$ form a complete orthonormal set of state vectors of the Hamitonian H^R with given angular momentum l; here α is a complete set of quantum numbers (apart from l) characterizing the given state. In accordance with the discussion in the previous section, we represent the Coulomb partial-wave "in" and "out" states in the form

$$|p_c^{(\pm)},\ l\rangle = (ip)^l\,[f_l^{(\pm)}(p)]^{-1}|p_c,\ l\rangle. \quad (17)$$

Using the completeness of the states $|\alpha,l\rangle$ and taking into account the relations (10)–(12) and (17), we obtain from Eq. (16) in the limit $R\to\infty$ a spectral representation for the renormalized amplitude $\tau_l(p',p;s)$ of the form

$$\tau_l(p',\ p;\ s) = w_l(p',\ p) - \sum_\alpha \frac{1}{\pi}\int_0^\infty ds'\tilde{\rho}_l(s')\,\frac{1}{\pi}\int_0^\infty ds''\tilde{\rho}_l(s'')\times w_l(p',\ \sqrt{s'})\,\frac{\Phi_{\alpha,l}(\sqrt{s'})\Phi^*_{\alpha,l}(\sqrt{s''})}{s-s_{\alpha,l}}\,w_l(\sqrt{s''},\ p), \quad (18)$$

where $\Phi_{\alpha,l}(p)=\langle p_c,l\,|\alpha,l\rangle$. The orthogonality condition for the functions $\Phi_{\alpha,l}(p)$ has the form

$$\frac{1}{\pi}\int_0^\infty \tilde{\rho}_l(s)\,\Phi_{l,\alpha}(\sqrt{s})\,\Phi^*_{l,\alpha'}(\sqrt{s})\,ds=\delta_{\alpha\alpha'}. \quad (19)$$

It follows from the spectral representation (18) that if the system has a bound state at $s=s_a$, then in the neighborhood of the point $s=s_a$

$$\tau_l(p',\ p;\ s)\cong -\frac{g_{\alpha,l}(p')\,g_{\alpha,l}(p)}{s-s_a}, \quad (20)$$

where the vertex function is

$$g_{\alpha,l}(p) = \frac{1}{\pi}\int_0^\infty w_l(p,\ \sqrt{s})\,\Phi_{\alpha,l}(\sqrt{s})\,\tilde{\rho}_l(s)\,ds. \quad (21)$$

At the same time, it follows from Eq. (13) and the expression (20) that the function $g_{\alpha,l}(p)$ satisfies the homogeneous equation

$$g_{\alpha,l}(p) = \frac{1}{\pi}\int_0^\infty w_l(p,\ \sqrt{s})\,g_{\alpha,l}(\sqrt{s})\,\frac{\tilde{\rho}_l(s)}{s-s_a}\,ds. \quad (22)$$

Comparing (21) and (22), we obtain the relation

$$\Phi_{\alpha,l}(p) = \frac{g_{\alpha,l}(p)}{p^2+\varkappa^2}. \quad (23)$$

For an interaction of the form (1), the vertex function $g_{\alpha,l}(p)$ as follows from Eq. (22) and the properties of the matrix elements $w_l(p,p')$, has a cut from $-\infty$ to $\varkappa_0^2$ with respect to the variable $s=p^2$. Note that the value of $g_{\alpha,l}(p)$ at the point $p=i\varkappa$ is directly related to the vertex constant $\tilde{G}_l$ by

$$\tilde{G}_l^2 = (-1)^l\,\frac{\pi}{\mu^2}\,(\varkappa)^{2l}g^2(i\varkappa). \quad (24)$$

4. GENERALIZATION OF THE K-MATRIX FORMALISM TO THE CASE OF COULOMB–NUCLEAR SCATTERING

In the theory of the nuclear reactions,[12] the K-matrix approach is used to unitarize the scattering amplitude. In Ref. 14, a dispersion derivation of the Heitler equation, which relates the K matrix to the scattering amplitude, was proposed. A similar method can be used to generalize this equation to take into account Coulomb effects. Indeed, as follows from Eq. (5), the imaginary part of the reciprocal amplitude $T_l^{-1}(s)$ does not depend on the dynamics of the strong interaction and is equal to $-\theta(s)\tilde{\rho}_l(s)$. Therefore, if the function $K_l^{-1}(s)$ is defined as the difference between $T_l^{-1}(s)$ and the dispersion integral along the right-hand cut,

$$-i\sigma_l(s) = s^l\left[\frac{s}{\pi}\int_0^\infty \frac{\tilde{\rho}_l(s')\,ds'}{(s')^{l+1}(s'-s-i\varepsilon)} + \sum_{n=0}^{l}\alpha_n\lambda^{2n}/s^n\right], \quad (25)$$

where α_n are certain subtraction constants, then the relationship between $K_l(s)$ and $T_l(s)$ will have the form of the Heitler equation

$$T_l(s) = K_l(s) + i\,K_l(s)\,\sigma_l(s)\,T_l(s). \quad (26)$$

The particular choice of the constants α_n corresponds to a certain method of defining the K matrix charged particles (in particular, these constants can be set equal to zero). The K matrix introduced in this manner is analytic in the neighborhood of the point $s = 0$ and contains only a dynamical left-hand cut. In Ref. 14, a nonsingular integral equation for the K matrix in the theory of potential scattering was formulated. In Ref. 15, a K-matrix approach with allowance for the Coulomb interaction was proposed on the basis of a generalization of the R-matrix formalism. Note that the K matrix introduced in Ref. 14 on the basis of the dispersion approach is not, in contrast to the K matrix considered in Ref. 15, a meromorphic function in the s plane, since for an interaction of the type (1) it is an analytic function with a dynamical left-hand cut.

In the formulation of the N/D equations and the K-matrix formalism given above, we considered for simplicity the case of single-channel scattering. However, these methods can be generalized to the many-channel case. One can introduce a renormalized matrix of the partial-wave amplitudes, $\hat{T}(s)$, this satisfying a matrix N/D representation $\hat{T}(s) = \hat{N}(s)\hat{D}^{-1}(s)$. For $\hat{N}(s)$ and $\hat{D}(s)$ one can write down matrix equations that have the same form as the single-channel equations, except that $L_l(s)$ must be replaced by a potential matrix $\hat{L}(s)$, and $\tilde{\rho}_l(s)$ by a diagonal matrix whose elements in channel α have the form $\tilde{\rho}_l(s_\alpha)$, where s_α is the square of the relative momentum of the particles in this channel. The K-matrix equation (26), in which $\sigma_l(s)$ must be replaced by a diagonal matrix with elements $\sigma_l(s_\alpha)$ in channel α, can be generalized similarly.

5. CALCULATION OF THE EFFECTS OF COULOMB–NUCLEAR INTERFERENCE ON THE BASIS OF DATA ON THE ENERGY DEPENDENCE OF THE PARTIAL-WAVE AMPLITUDES

In a number of problems involving charged particles (for example, in phase-shift analysis; see Ref. 16) it is necessary to separate the contribution of electromagnetic effects, among which the Coulomb effects are the most important at low and intermediate energies. It is expedient to take into account the Coulomb interaction nonperturbatively, whereas in the calculation of the remaining electromagnetic effects perturbation theory is sufficient. It is of great practical interest to develop methods of allowance for the Coulomb effects that are to a considerable degree model-independent, can be generalized fairly easily to the relativistic case, and are based solely on knowledge of the energy dependence of the partial-wave amplitudes on the energy shell. These problems have been discussed intensively in the literature in recent years. For example, a group of Austrian physicists have developed a method[17] in which the Coulomb–nuclear correction to the phase shift is calculated in terms of the phase shift and its derivative with respect to the energy when the Coulomb interaction is switched off. It should be noted that this correction to the phase shift and to the inelasticity parameter can be calculated in the first order in the fine-structure constant, and the method can be justified in the framework of the semiclassical approximation. This method was used, in particular, in one of the more recent phase-shift analyses of NN scattering.[18]

In this section, we consider a method of calculating the effects of Coulomb–nuclear interference based on the use of the N/D equations; we assume that we know the energy dependence of the partial-wave scattering amplitudes on the energy shell. We shall also assume that in general the scattering is inelastic. We demonstrate the method that we use to take into account the inelastic channels in the N/D equations with allowance for the Coulomb effects for the example of a separable energy-dependent potential. For simplicity, we restrict ourselves to a single-term separable interaction, and we shall assume that the renormalization of the functions $N(s)$ (which is determined by the contribution of the Coulomb effects on the dynamical cut) is given by an expression of the form (14). Thus, we assume that the function $\lambda(s)$, which determines the energy dependence of the separable potential, has a cut that begins at the threshold of the inelastic channels, s_1. Then the discontinuity of $T^{-1}(s)$ across C_R has the form

$$\operatorname{Im} T_l^{-1}(s) = -\tilde{\nu}_l(s) \equiv -\tilde{\rho}_l(s) + \frac{\operatorname{Im}\lambda_l^{-1}(s)}{N_l(s)}$$
$$= -[\rho_l(s)\,C_l^2(s) + \gamma_l(s)/\xi_l(s)], \quad (27)$$

where $\gamma_l(s) = -\operatorname{Im}\lambda_l^{-1}(s)/\bar{N}_l(s)$, and $\xi_l(s)$ is the factor of the Coulomb renormalization of the function $N_l(s)$ [see Eq. (14)]. Thus, when the Coulomb interaction is switched off, $\tilde{\nu}_l(s) \to \nu_l(s) \equiv \rho_l(s) + \gamma_l(s)$. As a result, to determine the function $N_l(s)$ we have a linear singular inhomogeneous equation of the form

$$N_l(s)\operatorname{Re} T_l^{-1}(s) = 1 - \frac{s-s_0}{\pi}\int_{C_R}\frac{\tilde{\nu}_l(s')\,N_l(s')}{(s'-s)(s'-s_0)}\,ds'. \quad (28)$$

Applying the well-known methods, we obtain a solution of Eq. (28) in the form (when there are no bound states)

$$N_l(s) = \frac{\sin\theta_l(s)}{\nu_l(s)}\exp[-W_l(s)], \quad (29)$$

$$W_l(s) = \frac{s-s_0}{\pi} P \int_{C_R} \frac{\theta_l(s')\, ds'}{(s'-s)(s'-s_0)}, \quad (30)$$

and the phase shift $\theta_l(s)$ is related to the phase shift $\delta_l(s)$ and the parameter $\eta_l(s)$ (in terms of which $T_l(s)$ has the form $[\eta_l(s)\exp(2i\delta_l(s)) - 1]/2i\rho_l(s)$:

$$\operatorname{ctg} \theta_l(s) = \frac{\sin 2\delta_l(s)}{1-\eta_l(s)\cos 2\delta_l(s)}, \quad (31)$$

and the function $\nu_l(s)$ can also be expressed in terms of the parameters $\delta_l(s)$ and $\eta_l(s)$:

$$\nu_l(s) = \frac{2\tilde{\rho}_l(s)(1-\eta_l(s)\cos 2\delta_l(s))}{1+\eta_l^2(s)-2\eta_l(s)\cos 2\delta_l(s)}. \quad (32)$$

We can now calculate $\delta_l^{(n)}$ and the inelasticity parameters $\eta_l^{(n)}$ when there is no Coulomb interaction by using the relation

$$\overline{T}_l = [\eta_l^{(n)} \exp(2i\delta_l^{(n)}) - 1]/2i\rho_l(s) = \overline{N}_l(s)/\overline{D}_l(s),$$

where $\overline{N}(s) = N_l(s)/\xi_l(s)$, and $\overline{D}_l(s)$ is calculated in accordance with

$$\overline{D}_l(s) = 1 - \frac{s-s_0}{\pi} \int_{C_R} \frac{\nu_l(s')\,\overline{N}_l(s')}{(s'-s)(s'-s_0)}\, ds'. \quad (33)$$

We make the following remarks about our procedure. Above, we used the model of a separable interaction with a form factor of Hulthén type (but in general with an energy-dependent parameter $\beta(s)$) only to particularize the form of the renormalization of the contribution from the dynamical cut [the facor $\xi(s)$]. Otherwise, Eqs. (27)–(28) are fairly general. In this connection, it must be emphasized that the Coulomb correction $\Delta L_l^{(c)}(s)$ to the potential function $\overline{L}_l(s)$, which reduces to a renormalization [$\overline{L}_l(s)$ is $\overline{L}_l(s)$ without the Coulomb interaction] of the function $\overline{N}_l(s)$, is due to forces of the same range as the short-range part of the interaction (since $\overline{L}_l(s)$ and $\Delta L_l^{(c)}(s)$ have the same domain of analyticity). Of course, the renormalization of the left-hand cut depends on the dynamics of the interaction. Nevertheless, we can specify an effective quantity $\beta_l(s)$ in the model of a separable interaction that determines the factor $\xi_l(s)$ in (14) by analyzing the specific physical mechanisms corresponding to the nearest singularities of the scattering amplitude with respect to the momentum transfer. The Coulomb renormalization of the spectral function $\rho_l(s)$ on the right-hand cut is determined by the penetrability factor $C_l^2(s)$ and is model-independent. The factor $C_l^2(s)$ contains the strongest Coulomb singularity as $s \to 0$, and therefore the renormalization of the right-hand cut determines largely, at least in the low-energy region, the effects of the Coulomb–nuclear interference.

6. NUMERICAL CALCULATIONS

The N/D equations have been used to calculate the phase shifts and differential cross sections of various processes with allowance for Coulomb effects.[8,19–23] To solve these equations, the discontinuities of the partial-wave scattering amplitudes across the dynamical cut, which determine the potential function $L_l(s)$, were specified with allowance for the contribution of the mechanisms corresponding to the closest singularities of the scattering amplitude with respect to the momentum transfer. For example,

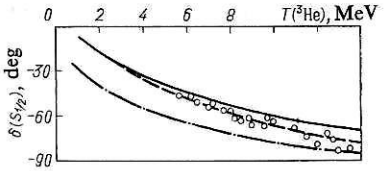

FIG. 1. Energy dependence of the $S_{1/2}$ phase shift in ^{3}He–^{4}He scattering. The points are the results of the phase-shift analysis of Ref. 25.

in the calculation of the energy dependence of the S-wave phase shift in ^{3}He–^{4}He scattering,[22] the potential function $L_l(s)$ was calculated with allowance for the contribution of the diagram corresponding to the neutron-transfer mechanism. The value of the vertex constant was $G^2(^4\text{He}$–$^3\text{He}n) = 12$ F, in agreement with the available data.[2] Note in particular that a recent analysis[24] of data on the charge form factor of the ^{4}He nucleus with allowance for the contribution of meson exchange effects agrees well with this value of the vertex constant: $G^2(^4\text{He}$–$^3\text{He}n) = 11.6$ F. The influence of the Coulomb effects on the dynamical cut in the N/D equations was taken into account by introducing a renormalization factor $\xi_l(s)$ in the function $N_l(s)$ [see Eq. (14)]. Allowance for the factor $\xi_l(s)$ partly compensates the influence of the renormalization of the contribution from the right-hand cut in the N/D equations. It follows from comparison of the results of the calculations with the data of phase-shift analysis[25] that allowance for the pole mechanism and the singularities associated with the vertex function leads in the calculation of $L_l(s)$ to a good description of the experimental data (continuous curve in Fig. 1). Nevertheless, we investigated the contribution of the more distant singularities corresponding to the mechanism of quasifree scattering of α particles by a bound nucleon in ^{3}He. Allowance for this mechanism improves somewhat the agreement between the theory and experiment (broken curve in Fig. 1). For comparison, Fig. 1 also shows the results of calculating the $S_{1/2}$ phase shift in ^{3}He–^{4}He scattering without the Coulomb interaction on the right- and left-hand cuts (chain curve) for the same case for which the included Coulomb interaction leads to the continuous curve.

The method was used to find the S-wave phase shift in ^{3}H–^{4}He scattering on the basis of data of phase-shift analysis of ^{3}He–^{4}He scattering. A similar method was used to calculate the energy dependence of the S phase shifts in p^3He and p^4He scattering. The results of the calculation agree well with the phase-shift analyses. For example, allowance for the deuteron-exchange mechanism in the calculation of the $^1S_0$ phase shift in p^3He scattering leads to good agreement with the phase-shift analysis.[26] The value of the vertex constant $\tilde{G}^2(^3\text{He}$–$pd)$ was taken to be 1.3 F, in agreement with the literature data.[2] Allowance was also made in the calculation for the mechanism of quasifree proton scattering by a bound nucleon of the ^{3}He nucleus, and a prediction for the energy dependence of the $^1S_0$ phase shift in n^3H scattering was obtained.[8]

The N/D equations and the K-matrix approach with allowance for Coulomb effects were used[19,20] to calculate the cross sections for scattering of K^+ mesons on the ^{2}H, ^{3}He,

TABLE I. Values of the vertex constant $\tilde{G}(^3\text{He}\text{–}pd)$, the nd doublet scattering length a_n, the difference ΔE between the binding energies of the ^{3}He and ^{3}H nuclei, and the difference $\Delta G^2 = G^2(^3\text{H}\text{–}nd) - \tilde{G}^2(^3\text{He}\text{–}pd)$ between the constants as a function of the parameter β.

β, F^{-1}	$\tilde{G}^2$, F	a_n, F	ΔE, MeV	ΔG^2, F
1	1.12	0.53	0.82	0.052
0.9	1.19	0.67	0.77	0.052
0.8	1.28	0.84	0.73	0.053

and ^{4}He nuclei. In this case, the partial-wave K matrix and the function $L_l(s)$ were calculated with allowance for the mechanism for quasifree scattering of the K^+ meson by a bound nucleon of the target nucleus.

Analysis of S-wave pd scattering by means of the N/D equations[21] was used to determine the vertex constant $\tilde{G}^2(^3\text{He}\text{–}pd)$. The potential function was calculated with allowance for the contribution of the pole diagram corresponding to the neutron-exchange mechanism. The contribution of the more distant singularities was approximated by a triangle diagram containing two free parameters—the vertex constant at the four-leg vertex and the Hulthén parameter β at the three-leg vertex (this parameter determines the cutoff of the discontinuity of the partial-wave amplitude across the left-hand cut). The first parameter was fixed by the condition that the amplitude have the correct position of the pole with respect to s corresponding to the bound state. The parameter β was determined by analyzing the data of low-energy nd scattering without the Coulomb interaction. The results of the calculation of the vertex constant $\tilde{G}^2(^3\text{He}\text{–}pd)$, the doublet and nd scattering length a_n, the difference ΔE betwen the binding energies of the ^{3}He and ^{3}H nuclei, and the difference $\Delta G^2 = G^2(^3\text{H}\text{–}nd) - \tilde{G}^2(^3\text{He}\text{–}pd)$ between the vertex constants are given in Table I. For $\beta = 0.9\ \text{F}^{-1}$, the values of G^2, a_n, and ΔE agree well with the experimental values [we recall that the experimental value of the doublet nd scattering length is 0.65 F (Ref. 27)]. The results of the calculation of the $^2S_{1/2}$ phase shift of pd scattering are shown in Fig. 2. The value of the doublet pd scattering length for $\beta = 0.9\ \text{F}^{-1}$ is 2.17 F. It follows from the data which we have given that the vertex constant $\tilde{G}^2(^3\text{He}\text{–}pd)$ is 0.05 F less than the constant $G^2(^3\text{He}\text{–}nd)$. This result is almost independent of the details of the approximation of the distant singularities on the left-hand cut.

The N/D equations with allowance for Coulomb effects can be used to extract information about the vertex constants of nuclei from data of a phase-shift analysis by analytic continuation of the partial-wave amplitude to the point of a pole corresponding to a bound state. If data of a phase-shift analysis are known in a sufficiently wide range of energies, the method described in Sec. 6 [see Eq. (30)] can be used for this purpose. If the data are more restrictive [i.e., if the data of the phase-shift analysis are insufficient for the direct recovery of the function $N_l(s)$ in accordance with Eq. (30)], some analytic approximation of the function $N_l(s)$ can be used. We illustrate this by the example of the calculation of the vertex constant $\tilde{G}(^7\text{Be}\text{–}^4\text{He}^3\text{He})$.[22] We represent the function $N_l(p',p;s)$, which determines the renormalized off-shell scattering amplitude, in separable form with a form factor of Hulthén type. The quantities λ and β, which determine the strength and effective range of the interaction, were assumed to be independent of the energy and were chosen by the χ^2 method in accordance with the $P_{3/2}$ phase shift of ^{3}He–^{4}He scattering.[25] It can be seen from Fig. 3 that this parametrization of the function $N_l(s)$ reproduces well the energy dependence of the $P_{3/2}$ phase shift. At the same time, the value of the vertex constant $\tilde{G}^2(^7\text{Be}\text{–}^4\text{He}^3\text{He})$ is 0.24 F.

The method which we have considered can be used effectively to determine model-independent parameters of resonance states. As an example, we consider the determination of the parameters of P-wave resonances in $p\alpha$ scattering.[23] It is known that the energies and widths of the near-threshold $P_{3/2}$ and $P_{1/2}$ resonances in $N\alpha$ scattering determined by means of different resonance formulas and, in particular, in R-matrix analysis contain large uncertainties and are strongly model-dependent.[28,29] Very important in this connection is a model-independent (i.e., based on the analytic properties of the S matrix) determination of the resonance parameters. In accordance with analytic S-matrix theory, a resonance corresponds to a pole of the partial-wave S matrix on the second sheet of the Riemann surface of the complex s plane, and its parameters are the position of the pole and the

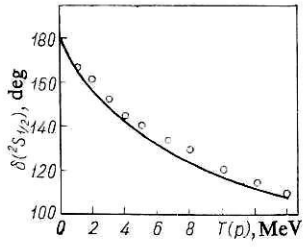

FIG. 2. Energy dependence of the $S_{1/2}$ phase shift in pd scattering. The points are the data of the phase-shift analysis of Ref. 28.

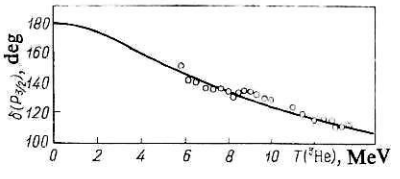

FIG. 3. Energy dependence of the $P_{3/2}$ phase shift in ^{3}He–^{4}He scattering. The points are the results of the phase-shift analysis of Ref. 25.

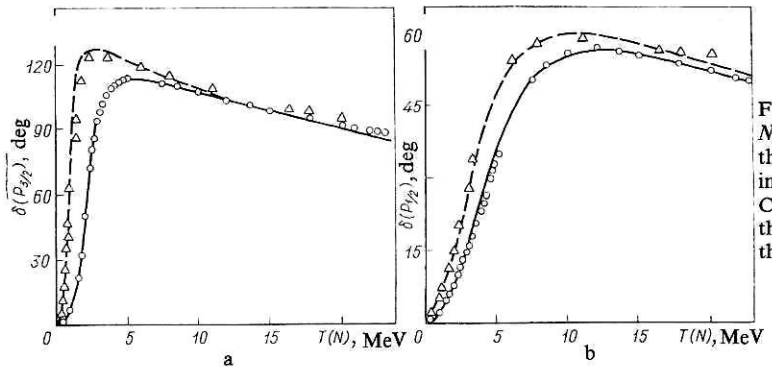

FIG. 4. Energy dependence of the $P_{3/2}$ (a) and $P_{1/2}$ (b) phase shifts in $N\alpha$ scattering. The continuous curves represent the calculation of the phase shifts in $p\alpha$ scattering with allowance for the Coulomb interaction; the broken curves represent the calculation with the Coulomb interaction switched off; the open circles are the data of the phase-shift analyses of $p\alpha$ scattering[31,32]; the open triangles are the data of the phase-shift analyses of $n\alpha$ scattering.[32,33]

residue of the S matrix at it (see, for example, Ref. 30). It should be emphasized that this is a universal and the most consistent way of determining resonance parameters, and it also applies for broad resonances. In the presence of the Coulomb interaction, we determine the vertex constant of a resonance on the basis of the same approach as was used above to determine the vertex constant for a bound state. Then the parameters of the bound and resonance states are determined in a unified manner. Besides the vertex constant $\tilde{G}_l$ [see (12)], it is convenient to consider the dimensionless constant R_l, which is related to the $T_l(s)$ residue in the k plane:

$$R_l = \mathrm{i}\,(-1)^{l+1} \lim_{k \to k_r} [(k-k_r)\, s^l T_l(s)], \tag{34}$$

where k_r determines the position of the resonance pole on the second sheet. In the case of a bound state, the constant R_l is real, positive, and related to $\tilde{G}_l^2$ by $\tilde{G}_l^2 = (-1)^l \cdot 2\pi\varkappa\mu^{-2}R_l$.[3)]

The data of phase-shift analyses of $p\alpha$ scattering[31,33] were used to determine the parameters of P-wave resonances for scattering in states with total angular momentum $j = 3/2, 1/2$, i.e., the constants R_j of the resonances and the positions of the poles on the second sheet corresponding to these resonances in the complex plane of the energy $E_{rj} = (k_{rj})^2/2\mu$. The function $N(s)$ was parametrized in the same form as was used above to describe ^{3}He–^{4}He scattering in the P wave, and the corresponding parameters λ and β were chosen by the χ^2 method on the basis of the experimental phase shifts of $p\alpha$ scattering.[31,32] As can be seen from Fig. 4, this parametrization (continuous curves) reproduces well the energy dependence of the $P_{3/2}$ and $P_{1/2}$ phase shifts in the region of energies $T = 0$–23 MeV of the incident proton. The results of the calculation of the constants $R_j \equiv |R_j| \exp(i\varphi_j)$ and the positions E_j of the resonance poles on the second sheet are given in Table II. The method makes it possible to calculate the phase shifts and the parameters of the resonances in $n\alpha$ scattering using the data of $p\alpha$ scattering. These quantities are calculated by formally switching off the Coulomb interaction for unchanged parameters λ and β. The results of this calculation for the phase shifts are shown by the broken curves in Fig. 4. It can be seen from Fig. 4 that the phase shifts with the Coulomb interaction switched off agree well with the phase-shift analysis of $n\alpha$ scattering.[32,33]

[3)]In Sec. 7, a different definition of the vertex constant of a resonance is used.

The vertex constants of the $P_{3/2}$ and $P_{1/2}$ resonances in $p\alpha$ scattering given in Table II were found in Ref. 23. The data in this table on the energies and widths of the resonances agree fairly well with the results of the analysis made in Ref. 29, in which these parameters were found from the position of the resonance pole on the second sheet. But there is a large difference between these data and the results of the R-matrix analysis of Ref. 34. The parameters of the $n\alpha$ resonances given in Table II were obtained on the basis of $p\alpha$ scattering data. These results also agree with the data of Refs. 29 and 35, in which the parameters were determined from the data of $n\alpha$ scattering.

7. CHARGED-PARTICLE STRIPPING REACTIONS TO RESONANCE STATES

In this section, we apply the dispersion approach to analyze the reactions of stripping of charged particles to resonance states of the final nuclei. It is well known that when the amplitudes of these reactions are calculated in the DWBA serious difficulties are encountered in the calculation of the radial integrals, which diverge at the upper limit.[36] In Ref. 37, a dispersion method was proposed for calculating neutron stripping to resonance states that is free of the difficulties that arise in the DWBA. In the dispersion method, the differential cross section of the reaction is parametrized directly in terms of the resonance width Γ, which is determined by comparing the calculated and measured cross sections. In addition, the dispersion approach makes it possible to calculate equally easily stripping reactions to resonance states described by both simple and more complicated, for example, two-step, mechanisms.[38]

Coulomb part of the vertex form factor for decay of a resonance state to two charged particles

We give without rigorous derivation an expression for the Coulomb part of the vertex form factor corresponding to decay of the resonance state of a nucleus B^* to two charged particles A and a: $B^* \to A + a$. The general expression for the vertex form factor of the decay of the resonance state can be written in the form

$$G(l_r j_r;\, q) = (q/q_r)^{l_r}\, G(l_r j_r)\, g(l_r j_r;\, q^2), \tag{35}$$

where $g(l_r\, j_r; q^2)$ is the reduced vertex form factor, which can be represented as the sum of a Coulomb and a Coulomb–nuclear term.[2] The Coulomb part is

TABLE II. Parameters of P-wave resonances in $N\alpha$ scattering.

Nucleus	jP	Re E_{rj}, MeV	Im E_{rj}, MeV	$\lvert R_j \rvert$	φ_j, deg
^{5}Li; $p\alpha$	$3/2^-$	1,655	0,639	0,304	−135.5
	$1/2^-$	2,691	3,224	0,313	−177.9
^{5}He; $n\alpha$	$3/2^-$	0,697	0,271	0,160	132,3
	$1/2^-$	1,875	2,648	0,237	177.1

lomb and a Coulomb–nuclear term.[2] The Coulomb part is

$$g^{(C)}(l_r;\ q^2) = \exp(\pi\eta_r/2)\frac{2(l_r+1)!}{\Gamma(l+1+i\eta_r)}(q^2-q_r^2)^{l_r+i\eta_r}\int_0^\infty dt\, t^{l_r+i\eta_r}(t-2iq_r)^{l_r-i\eta_r}[(t-iq_r)^2+q^2]^{-l_r-2}(t-iq_r). \tag{36}$$

In (35) and (36), we have introduced the following notation: l_r and j_r are the orbital and total angular momenta of particle a at the vertex $B^* \to A + a$; q is the relative momentum of particles a and A; $q_r = (2\mu_{Aa}E_r)^{1/2}$; $E_r = E_0 - i\Gamma/2$; $\eta_r\mu_{Aa}Z_AZ_ae^2/q_r$; E_0 and Γ are the energy and total width of the resonance state of the nucleus B^*; $\mu_{\alpha\beta} = m_\alpha m_\beta/(m_\alpha + m_\beta)$; m_α and $Z_\alpha e$ are the mass and charge of particle a; and $G(l_r\, j_r)$ is the vertex constant.[2] In the case of a narrow resonance ($\Gamma \ll E_0$), we can set $q_r \approx q_0 = (2\mu_{Aa}E_0)^{1/2}$, $\eta_r \approx \eta_0 = \mu_{Aa}Z_AZ_ae^2/q_0$.

With regard to the expressions (35) and (36) we note the following. In Ref. 39, an expression was found for the Coulomb part of the vertex form factor corresponding to the virtual decay $B \to A + a$ of a nuclear-stable state of the nucleus B to charged particles A and a. The expressions (35) and (36), which determine the Coulomb part of the vertex form factor for real decay of the resonance state, can be obtained from expressions (13) and (15) of Ref. 39 by replacing ϵ in them by $-E_r$ ($\varkappa$ by $-iq_r$), where $\epsilon = \varkappa^2/2\mu_{Aa} = m_A + m_a - m_B$ is the binding energy of the nucleus B with respect to virtual decay into A and a.

The vertex form factor for the virtual decay of the bound state $B = A + a$ is determined by[39]

$$G(lj;\ q) = -(\sqrt{\pi}/\mu_{Aa})(q^2+\varkappa^2)\int_0^\infty \varphi_{lj}(r) j_l(qr)\, r^2 dr, \tag{37}$$

where $j_l(x)$ is a spherical Bessel function. The vertex form factor for real decay of the resonance state is defined similarly. At the same time, it is necessary to replace $\varkappa^2$ in (37) by $-q_r^2$, and instead of $\varphi_{lj}(r)$ to take the Gamow wave function $\varphi_{l_rj_r}(r)$, which increases exponentially as $r \to \infty$. To give a meaning to the integral, it must be regularized by, for example, introduction of a factor $\exp(-\beta r^2)$ with $\beta \to 0$.[40] As a result, for the vertex form factor in the case of the resonance state we obtain

$$G(l_rj_r;\ q) = -(\sqrt{\pi}/\mu_{Aa})(q^2-q_r^2)\lim_{\beta\to+0}\int_0^\infty dr r^2 \exp(-\beta r^2)\varphi_{l_rj_r}(r)\, j_{l_r}(qr). \tag{38}$$

The Coulomb part of the vertex form factor for the decay of the resonance state into the two charged particles takes into account the contribution to $G(l_r\, j_r; q)$ from the "Coulomb" cut in the q^2 plane from $q^2 = q_r^2$ to ∞, and is obtained by substituting in (38) in place of $\varphi_{lrjr}(r)$ the function $c_{l_rj_r}r^{-1} - W_{-i\eta_r, l_r+1/2}(2iq_r r)$, where $W_{\lambda,\nu}(x)$ is a Whittaker function,[41] and $c_{l_rj_r}$ is an asymptotic coefficient related to the vertex function by

$$G(l_rj_r) = -\exp\left[i\pi\left(\frac{l_r+i\eta_r}{2}\right)\right](\sqrt{\pi}/\mu_{Aa})c_{l_rj_r}. \tag{39}$$

The analogous relation for a bound state is obtained by the substitution $\eta_r \to -i\eta$, $q_r \to i\varkappa$, $c_{l_rj_r} \to c_{lj}$, where c_{lj} and η are the asymptotic coefficient and Coulomb parameter of the bound state.[2] In Ref. 42, it was shown that the residue at the pole of the elastic-scattering S matrix is related to $c_{l_rj_r}$ by

$$A_{l_rj_r} = -i(-1)^{l_r}\exp(-\pi\eta_r)\, c_{l_rj_r}^2. \tag{40}$$

Since $A_{l_rj_r}$ can be expressed in terms of $\gamma = \Gamma/(2E_0)$,[42] it follows that $c_{l_rj_r}$ is directly related to the width $\Gamma(l_r\, j_r)$ of the resonance for decay through the channel $(aAl_r\, j_r)$. In the case of a narrow resonance, to terms of order γ we have[42]

$$c_{l_rj_r}^2 = [\mu_{Aa}\Gamma(l_rj_r)/q_0]\exp(2i\delta_{l_rj_r}(q_0) - i\pi l + \pi\eta_0),$$

where $\delta_{l_rj_r}$ is the shift of the nonresonance scattering. A rigorous derivation of (36) is given in Ref. 43.

Differential cross section for charged-particle stripping to a resonance state

We consider the stripping reaction

$$A\ (x,\ y)\ B^*\ (a)A \tag{41}$$

and assume that it takes place in two stages—first stripping of the charged particle a to a resonance state of the nucleus B, and then decay of the two resonance states into the two particles A and a (Fig. 5). We restrict the treatment to narrow isolated resonances that decay only through the elastic channel ($B^* \to A + a$).

Then, as is shown in Ref. 37, the differential cross sec-

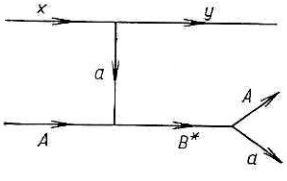

FIG. 5. Feynman diagram describing the reaction mechanism of stripping of the charged particle a to the resonance state B^* of the final nucleus.

TABLE III. Results of the analysis of the angular distributions of the stripping reaction on light nuclei.

Reaction	Residual nucleus	Exc. energy of resonance state, MeV	Information about res. state from elastic scattering of protons			$\epsilon_{x\,\mathrm{lab}}$, MeV	η_0	η_i	η_f	Γ, keV	
			l_r	J^π	Γ, keV					with allowance for the Coulomb interaction	without it
d, n	^{8}Be	17.84	1	1^+	10.7±0.5	9.75	0.71	0.21	0	$19.4^{+13.2}_{-4.1}$	94.6
	^{8}Be	18.14	1	1^+	147	9.75	0.47	0.21	0	118^{+72}_{-23}	$2.31\cdot10^2$
	^{13}N	2.37	0	$1/2^+$	35±1	11.8	1.39	0.39	0	30	$1.91\cdot10^3$
	^{13}N	2.37	0	$1/2^+$	35±1	15.25	1.39	0.34	0	41	$2.4\cdot10^3$
	^{21}Na	4.47	2	$3/2^+$	22	6.12	1.08	0.90	0	10−35	222
	^{15}O	7.752	0	$1/2^+$	1.6±0.5	5.6	2.09	0.66	0	0.8	$1.7\cdot10^3$
	^{15}O	7.752	0	$1/2^+$	1.6±0.5	6.0	2.09	0.64	0	1.2	$1.7\cdot10^3$
^{3}He, d	^{13}N	2.37	0	$1/2^+$	35±1	16	1.39	0.82	0.55	34.2	$2.5\cdot10^3$
						17	1.39	0.79	0.53	28	$1.7\cdot10^3$
						18	1.39	0.77	0.50	24.8	$1.6\cdot10^3$
	^{19}F	8.795	0	$1/2^+$	26	16	1.34	1.09	0.70	$16.5^{+9.8}_{-6.1}$	$4.1\cdot10^2$
	^{19}F	10.267	2	$3/2^+$	11	16	0.81	1.09	0.78	$14.4^{+1.7}_{-8.9}$	24.3
	^{19}F	10.33	2	$3/2^+$	5.2	16	0.80	1.09	0.79	$9.8^{+11.3}_{-5.2}$	15.7

Note. References to the papers from which the experimental data and the information about the resonance state are taken are given in Ref. 43.

tion of the reaction (41) in the center-of-mass system, integrated over all the kinematic variables except the emission angle of particle y, is equal to the differential cross section of the binary reaction $A(x,y)B^*$, which is the first stage in the process (41). In Ref. 37, an expression was obtained for the differential cross section of neutron stripping to resonance states. The case when a charged particle is transferred requires a modification of the expressions of Ref. 37. We have analyzed the reactions (d,n) and $(^3\mathrm{He}, d)$. In the reaction (d,n), the Coulomb interaction in the three-leg vertex $d\to n+p$ is absent, and in the reaction $(^3\mathrm{He}, d)$ the Coulomb interaction at the vertex $^3\mathrm{He}\to d+p$ can be ignored because the Coulomb parameter at this vertex is small ($\eta\sim0.1$). Therefore, for these reactions we shall consider the Coulomb effects only at the vertex $A+a\to B^*$.[4)] In addition, we take into account approximately the effects of Coulomb–nuclear xA and yB^* scattering in the initial and final states (since the resonance state of the nucleus B is assumed to be narrow, the scattering of y by B^* can be treated as scattering by the stable nucleus B).

The differential cross section of the reaction $A(x,y)B^*$ was calculated in the framework of the dispersion peripheral model of Ref. 37, in which the reaction amplitude is expanded with respect to partial waves and the contribution from the lowest partial waves is completely ignored. In the peripheral partial-wave amplitudes that are taken into account, the effects of the distortions in the initial and final states were taken into account in the diffraction model of Ref. 43. An explicit expression for the differential cross section of the reaction $A(x,y)B^*$ in the case when charged particles (protons) are transferred was given in Ref. 43, which took into account the results of Ref. 37.

[4)]It is shown in Ref. 44 that in stripping reactions the contribution to the nuclear vertex form factors from nuclear breakup can be ignored.

Comparison with experiment

Numerical calculations were made for the reactions (d,n) and $(^3\mathrm{He},d)$; data are given in Table III. For these reactions, the differential cross section in the center-of-mass system, integrated over all the kinematic variables except the emission angle of the neutrons or deuterons, has the form[37]

$$\frac{d\sigma}{d\Omega}=(2J+1)\,\Gamma G_x^2\sigma\,(E_i,\,z). \tag{42}$$

Here, $G_x^2=0.43$ and 1.34 F are the vertex constants for the decays $d\to n+p$ $(x=d)$ and $^3\mathrm{He}\to p+d$ $(x=^3\mathrm{He})$, respectively,[2] and $\sigma(E_i,z)$ is a known function of $z=\cos\theta$ (θ is the scattering angle of the emitted neutrons or deuterons in the center-of-mass system) and E_i. The phases in the initial and final scattering states were calculated by the optical model.

It follows from (42) that the differential cross section of the reaction is proportional to $(2J+1)\Gamma$, which can be deter-

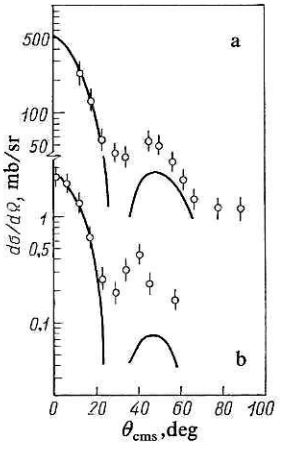

FIG. 6. Differential cross section of the reaction $^{12}\mathrm{C}(d,n)^{13}\mathrm{N}(2.37\ \mathrm{MeV};\ 1/2^+)$: a) $E_d=11.8$ MeV; b) $E_d=15.25$ MeV.

mined by comparing the calculated and experimental differential cross sections. In our calculations, the value of the factor $(2J+1)\Gamma$ and the cutoff parameters L and L' for the orbital angular momenta in the entrance and exit channels, respectively, were chosen to achieve the best fit of the calculated differential cross sections to the experimental cross sections and were determined from the minimum of χ^2.

As an illustration, some of the calculated angular distributions are given in Fig. 6. It can be seen that the theoretical angular distributions reproduce well the experimental distributions in the region of the principal (stripping) peak and correctly reproduce the shape of the experimental angular distributions outside the principal peak, though in absolute magnitude the differential cross sections in this region are lower than the experimental ones. In this connection, it must be emphasized that in our calculations we took into account the simplest mechanism of formation of the resonance state (see Fig. 5), which has the singularity in z nearest the physical region and therefore makes the main contribution to the reaction amplitude in the region of the principal maximum. But in the region of the minima and the following peaks an important contribution is made by more complicated mechanisms with singularities in z more distant. We have not taken into account these mechanisms here, and we therefore cannot expect good agreement between the calculated and experimental angular distributions. The main thing is to achieve the best agreement in the region of the principal peak, which gives the entire spectroscopic information about the resonance state. We note that in general the shape of the angular distribution does not depend strongly on l_r. However, the absolute value of $\sigma(E_i,z)$ is very sensitive to the values of l_r, and this makes it possible for a known value of the width Γ, obtained from analysis of elastic-scattering data, to determine l_r uniquely, or vice versa. To demonstrate the predictive power of the theory, we here determined the total widths Γ of resonance states using the values of l_r and the spin and parity J^π of the resonance state known from independent experiments on elastic scattering of protons by the corresponding target nuclei. The results of the analysis are given in Table III. The uncertainties in the values of Γ were obtained as a result of a variation of L and L' for which the calculated angular distributions describe the experimental distributions in the region of the principal peak (with allowance for the errors).

The calculations show that the Coulomb effects hardly influence the nature of the angular distributions but strongly increase $\sigma(E_i,z)$, this leading to a decrease in the value of Γ determined from the analysis. Allowance for the Coulomb effects in the initial and final states increased the cross section in the reactions which we considered. In this connection, we note that in stripping reactions to bound states such corrections reduce the absolute value of the cross section as a rule. But for sufficiently low binding energy ϵ at the vertex $A + a \to B$ in the considered range of energies the Coulomb effects in the initial and final states begin to increase the cross section, and for stripping reactions to resonance states, for which $\epsilon < 0$, this increase may reach a factor 2. But the values of $\sigma(E_i,z)$ are particularly sensitive to the value of the Coulomb parameter η_0 at the vertex $A + a \to B^*$. The influence of the Coulomb interaction at the vertex is much greater than the influence of the Coulomb effects in the initial and final states. Thus, for the resonance state (7.752 MeV) of the ^{15}O nucleus, which has the greatest value $\eta_0 = 2.09$ of all the resonance states that we analyzed, allowance for the Coulomb vertex effects increases $\rho(E_i,z)$ by almost three orders of magnitude. Thus, the combined allowance for the Coulomb effects in the three-leg vertex for the production of the resonance state and the Coulomb effects in the initial and final states always increased the cross section $\sigma(E_i,z)$, and this decreased the value of Γ determined from the analysis.

8. ANALYTIC PROPERTIES OF NONRELATIVISTIC DIAGRAMS WITH ALLOWANCE FOR COULOMB INTERACTIONS

Besides the traditional methods, for example, the DWBA, the dispersion approach, which was first proposed by Shapiro,[45] had also been used successfully to analyze nuclear reactions (see Ref. 2 and the reference given there). This approach is based on the idea that the singularities of the reaction amplitude with respect to $z = \cos\theta$ (θ is the *c.m.s.* scattering angle) nearest the physical region play a dominant part. The amplitude can be represented as an infinite series of nonrelativistic Feynman diagrams, and the problem of finding its nearest singularities reduces to that of finding the singularities of the simplest diagrams. The analytic properties of the various skeleton diagrams, i.e., the diagrams with constant vertices, have been investigated on many occasions (see, for example, Ref. 46 and the literature quoted there). As a rule, when the diagrams are made more complicated by including nuclear interactions between the particles, the singularities with respect to z move further away from the physical region, and therefore in the actual calculation of the amplitudes of nuclear reactions in the dispersion approach it is assumed that it is sufficient to taken into account the contribution of only the simplest diagrams. A different situation arises in the case of processes with charged particles.

The inclusion in the diagrams of three- and four-leg Coulomb vertices[5)] does not shift the singularities of the original diagram. But it follows from this that on the basis of an arbitrary original diagram describing the process under consideration one can construct an infinite series of diagrams containing all possible Coulomb rescatterings of the internal particles of the original diagram, and all these diagrams will have a singularity with respect to z wherever the original diagram does, and they must therefore be taken into account in the calculation of the reaction amplitude. This is the main feature of processes with charged particles.

In this section, we consider the analytic properties of nonrelativistic diagrams with allowance for Coulomb interactions between the particles. We formulate some general theorems that determine the change in the analytic properties of the original diagrams when the Coulomb vertices are

[5)]The three-leg vertices in the diagram describe the virtual or real decay (or synthesis) of a nucleus into two particles, while the four-leg vertices describe the scattering of two particles.

added, taking for simplicity as original diagrams only skeleton diagrams, i.e., diagrams with constant three- and four-leg vertices. Allowance for the Coulomb–nuclear vertices in the original diagrams does not influence the results.

Positions of the singularities of Feynman diagrams with Coulomb vertices

Let L be an arbitrary original (connected) nonrelativistic diagram with n internal lines and v vertex parts describing a binary reaction, and let L_C be the modified diagram obtained from L by including Coulomb vertices. The amplitude M_L of the diagram L depends on two invariant kinematic variables, which we can, for example, take to be the total kinetic energy E_i of the colliding particles in the center-of-mass system and z. Omitting for brevity the proof, we state an important theorem, which determines how the analytic properties of the diagram L change when the Coulomb interactions are included.

THEOREM 1. On the inclusion of a Coulomb interaction between particles 1 and 2 of diagram L, the positions of the intrinsic singularities[6] of diagram L are not changed, i.e., these singularities are common singularities of the diagrams L and L_C.[7]

This theorem is valid both in the case when one adds a four-leg Coulomb vertex describing the scattering of particles 1 and 2 and in the case when the Coulomb effects are taken into account in the three-leg vertex $3 \rightleftarrows 1+2$.

Behavior near singularities with respect to z of diagrams with allowance for Coulomb interactions

Allowance for Coulomb Interaction in the Initial and (or) Final State. We shall show how the nature of the singularities with respect to z of the diagram L changes when allowance is made for Coulomb scattering in the initial and (or) final state. The amplitude of the modified diagram L_C obtained from L including Coulomb scattering in the initial state is given by[47]

$$M_{L_C}(\mathbf{k}_f,\ \mathbf{k}_i) = \int \frac{d\mathbf{p}}{(2\pi)^3} M_L(\mathbf{k}_f,\ \mathbf{p})\, \Psi^{(C)(+)}_{\mathbf{k}_i}(\mathbf{p}), \tag{43}$$

where $M_L(\mathbf{k}_f,\mathbf{p})$ is the half-off-shell (with respect to the momentum $\mathbf{p}$) amplitude of the diagram L, $\Psi^{(C)(+)}_{k_i}(\mathbf{p})$ is the Fourier transform of the continuum Coulomb wave function in the momentum representation,[48] and $\mathbf{k}_i$ and $\mathbf{k}_f$ are the relative momentum of the particles in the initial and final states. Let ζ be an intrinsic singularity with respect to z of the amplitude $M_{L_C}(\mathbf{k}_f,\ \mathbf{k}_i)$ on the energy shell. By Theorem 1, the amplitude $M_{L_C}(\mathbf{k}_f,\ \mathbf{k}_i)$ also has a singularity at $z=\zeta$. We wish to find the behavior of M_{L_C} as $z\to\zeta$ when we know the behavior near this singularity of the amplitude M_L. For this, we expand $M_{L_C}(\mathbf{k}_f,\mathbf{k}_i)$ and $M_L(\mathbf{k}_f,\mathbf{k}_i)$ in partial waves and consider the on-shell partial-wave amplitude of the diagram L_C:

$$M_{L_C l}(k_f,\ k_i) \equiv M_{L_C l}(E_i) = \exp(i\sigma_l^{(i)}) \int_0^\infty \frac{dp}{2\pi^2}\, p^2 M_{Ll}(k_f,\ p)\, \Psi^{(C)}_{lk_i}(p). \tag{44}$$

Here, $M_{Ll}(k_f,p)$ is the half-off-shell partial-wave amplitude of diagram L, $\sigma_l^{(i)}$ are the Coulomb scattering phases in the initial state, and $\Psi^{(C)}_{lk_i}(p)$ is the partial-wave Coulomb wave function in the momentum representation, an explicit expression for which was obtained in Refs. 47 and 49. In accordance with the asymptotic theory of Ref. 50, the behavior of the partial-wave amplitudes of the diagram as $l\to\infty$ and the nature of its singularity with respect to z nearest the physical region stand in a direct relation to each other. Therefore, knowing $M_{L_C l}(E_i)$ in the limit $l\to\infty$, we can find the behavior of $M_{L_C}(E_i,z)\equiv M_{L_C}(\mathbf{k}_f,\mathbf{k}_i)$ near the nearest singularity with respect to z. Let φ be the singularity with respect to z of the amplitude $M_L(E_i,z)$ that is nearest the physical region. Then as $l\to\infty$ and $p\to k_i$ we have (Ref. 50)[8]

$$M_{Ll}(k_f,\ p) \approx C(k_f,\ p)\, \varepsilon_\chi l^{-(\chi+3/2)} \sqrt{\frac{\pi}{\tau^2-1}}\, (\zeta^2-1)^{(\chi+1)/2} \times \exp(-l\ln\tau), \tag{45}$$

$$\tau = \zeta - \sqrt{\zeta^2+1},\quad \chi = (3n-4v+3)/2,\qquad \varepsilon_\chi = \begin{cases} 1/\Gamma(-\chi), & \chi \neq 0,\ 1,\ 2\ \ldots, \\ (-1)^\chi \chi!, & \chi = 0,\ 1,\ 2\ \ldots; \end{cases} \tag{46}$$

where C is a preexponential factor that determines the power of the singularity and depends on the type of diagram. If ζ is not the nearest singularity, the expression (45) is still valid after separation from $M_L(\mathbf{k}_f,\mathbf{k}_i)$ of the contribution of the singularities with respect to z that are nearer than ζ. The asymptotic expression as $l\to\infty$ for $\Psi^{(C)}_{lk_i}(p)$ is given by

$$\Psi^{(C)}_{lk_i}(p) \approx -\frac{2\pi}{k_i p}\exp(-\pi\eta_i/2)\sqrt{\frac{\pi}{l}} \lim_{\gamma\to+0} \frac{d}{d\gamma}\left\{\left[\frac{p^2-(k_i+i\gamma)^2}{p^2-(k_i-i\gamma)^2}\right]^{\frac{i\eta_i}{2}} \times \exp(-l\ln\tau_\gamma(k_i,\ p))/(\tau_\gamma^2(k_i,\ p)-1)^{1/2}\right\}, \tag{47}$$

where $\tau_\gamma(k_i,p)$ and $\zeta_\gamma(k_i,p)$ are related by (46), and $\zeta(k_i,k) = (k_i^2+p^2+\gamma^2)/2k_i p$. Substituting (45) and (47) in (44), we can calculate the integral in the limit $l\to\infty$ by the method of steepest descent. It is convenient to begin by calculating the integral and then differentiating with respect to γ, and after that going to the limit $\gamma\to 0$. As a result, we obtain the leading term in the asymptotic expansion of $M_{L_C}(E_i)$ with respect to l^{-1} as $l\to\infty$:

$$M_{L_C l}(E_i) \approx \rho(E_i) l^{i\eta_i} M_{Ll}(E_i), \tag{48}$$

where we have used the relation $\exp(i\sigma_l^{i\eta_i}) \approx l^{i\eta_i}$, $l\to\infty$ and η_i is the Coulomb parameter in the initial state. The explicit form of $\rho(E_i)$ is here not important for us; the main thing is

[6] An intrinsic singularity of a diagram is one in which the poles of the propagators of all the internal particles participate in its formation.

[7] For brevity, we speak of the singularities of a diagram, meaning by this the singularities of its amplitude.

[8] By virtue of the properties of $\Psi^{(C)}_{lk_i}(p)$,[47] the main contribution to the integral (44) as $l\to\infty$ is made by the neighborhood of the point $p=k_i$, and therefore it is sufficient to know the behavior as $l\to\infty$ of the amplitude $M_{Ll}(E_i)\equiv M_{Ll}(k_f,k_i)$.

that it does not depend on l. It can be seen by comparing (48) and (44) that in the limit $l\to\infty$ the convolution of the generalized function $\Psi^{(C)}_{lk_i}(p)$ with the function $M_{L_l}(k_f,p)$, which is regular at $p=k_i$, reduces the multiplication of $M_{Ll}(E_i)$ by $\rho(E_i)$. The transition to the energy shell as a result of the integration of $M_{Ll}(k_f,p)$ is due to the fact that in the limit $l\to\infty$ the support of $\Psi^{(C)}_{lk_i}(p)$ is concentrated at $p^2=k_i^2$—the saddle point in (44) is given by the expression $p^2=k_i^2+O(\gamma)$.

In accordance with Ref. 50, the nature of the nearest singularity with respect to z of the amplitude $M_{L_C}(E_i,z)$ is determined by the dependence on l at large l of its partial-wave amplitudes $M_{L_Cl}(E_i)$, and therefore the appearance of the factor $l^{i\eta_i}$ in (48) changes the nature of the singularity ζ of the amplitude $M_L(E_i,z)$. Using the expressions of Ref. 50, we obtain from (48) and (45) the leading singular terms of $M_{L_C}(E_i,z)$ and $M_L(E_i,z)$ as $z\to\zeta$:

$$M^{(s)}_{L_C}=\rho(E_i)\,\Gamma(i\eta_i-\chi)\,\varepsilon_\chi(\zeta^2-1)^{i\eta_i/2}C(E_i)(\zeta-z)^{\chi-i\eta_i}, \tag{49}$$

$$M^{(s)}_{L}=C(E_i)(\zeta-z)^{\chi},\quad \chi\neq 0,\,1,\,2\ldots, \tag{50a}$$

$$M^{(s)}_{L}=-C(E_i)(\zeta-z)^{\chi}\ln(\zeta-z),\quad \chi=0,\,1,\,2\ldots, \tag{50b}$$

$$C(E_i)\equiv C(k_f,k_i).$$

It can be seen from (49) and (50) that allowance for the Coulomb interaction in the initial state does not change the positions of the singularities with respect to z of the original diagram L, but does change the nature and power of these singularities. The change in the power is due to the appearance of the factor $\rho(E_i)\Gamma(i\eta_i-\chi)\epsilon_\chi(\zeta^2-1)^{i\eta_i/2}$. When allowance is made for the Coulomb interaction in the final state or simultaneously in the initial and finals states, it is necessary to replace η_i in (48) and (49) by η_f or $\eta_i+\eta_f$, respectively (η_f is the Coulomb parameter in the final state).

Allowance for Coulomb Scattering of Internal Particles. **THEOREM 2.** The nature of the intrinsic singularities with respect to z of the diagram L is not changed by including Coulomb scattering of two internal particles 1 and 2.[9)]

Proof. Allowance for Coulomb scattering of particles 1 and 2 is equivalent to replacing the free Green's function G_0 of these particles by the Coulomb Green's function G_C. The spectral expansion of the partial-wave Coulomb Green's function G_{Cl} is given by an integral that contains a product of complex-conjugate partial-wave Coulomb Green's functions. At the same time, the phase factors $\exp(i\sigma_l)$, which change the nature of the singularities with respect to z when a Coulomb interaction is included in the initial and (or) final state, cancel. And in the limit $l\to\infty$ it follows by virtue of the properties of the partial-wave Coulomb wave functions that $G_{Cl}=NG_{0l}$, where the renormalization factor N depends on the blocks of the diagrams L with which G_{Cl} is contracted [this result is a consequence of (48)]. Thus, allowance for the Coulomb scattering of two internal particles of the diagram at large orbital angular momenta of the relative motion of these particles reduces to a simple renormalization of the partial-wave free Green's function of these particles, and this changes neither the positions nor the nature of the intrinsic singularities with respect to z of the diagram, but merely changes their power.

So far we have taken as initial diagrams only skeleton diagrams, but the results are not changed if the original diagrams already contain two-particle Coulomb Green's functions. It follows from this that the replacement of the three-particle free Green's function by the three-particle Coulomb Green's function corresponding to allowance for the Coulomb interaction of three particles in the intermediate state also changes neither the positions nor the nature of the intrinsic singularities with respect to z of the original diagram L, but does change their power.

Allowance for Three-Leg Coulomb Vertices. We state without proof a theorem.

THEOREM 3. Allowance for the three-leg Coulomb vertex $3\rightleftarrows 1+2$ changes both the nature and the power of the intrinsic singularities with respect to z of the diagram L.

The leading singular term in the amplitude of the modified diagram L_C as $z\to\zeta$ (ζ is an intrinsic singularity with respect to z of the diagram L) is given by the expression [cf. (50)]

$$M^{(s)}_{L_C}(\mathbf{k}_f,\mathbf{k}_i)=\tilde{C}(E_i)(\zeta-z)^{\chi+\eta_{12}}, \tag{51}$$

where $\eta_{12}=Z_1Z_2e^2\mu_{12}/\varkappa_{12}$ is the Coulomb parameter at the vertex $3\rightleftarrows 1+2$, χ is determined by the expression (46), and the coefficient $\tilde{C}$ determines the power of the singularity ζ.

9. SINGULAR PART OF THE TRANSFER-REACTION AMPLITUDE IN A MODEL OF THREE CHARGED PARTICLES

We consider the transfer reaction

$$(\beta\gamma)+\alpha\to\beta+(\alpha\gamma), \tag{52}$$

where $(\beta\gamma)$ is a bound state of particles β and γ; it is assumed that all three particles α, β, and γ have the same charge. Without loss of generality, the spins of the particles can be ignored, since the Coulomb effects in which we are interested do not depend on the spins.

The diagram of Fig. 7a determines the simplest mechanism of the reaction (52), which has at $z=\zeta$ the singularity

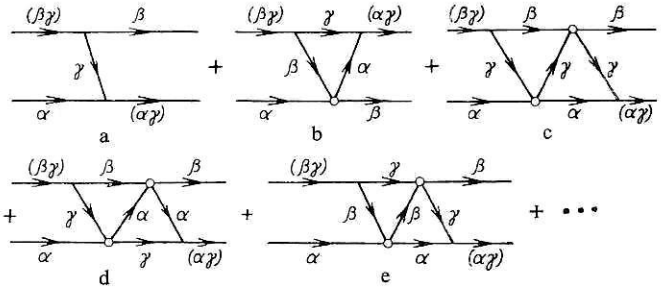

FIG. 7. Infinite series of diagrams taking into account all possible successive Coulomb rescatterings of particles α, β, and γ in the intermediate state and describing the transfer reaction mechanism for the charged particle γ in the three-body model. The open circles represent the four-leg Coulomb vertices.

[9)]This proposition is also valid when one of the particles 1 and 2 is an external particle and the other is internal, or both are external particles but one particle refers to the initial state and the other to the final state.

nearest the physical region:

$$\zeta = (k_i^2 + k_{f1}^2 + \varkappa_{\alpha\gamma}^2)/2k_ik_{f1}, \tag{53}$$

where $z = -\mathbf{k}_i\cdot\mathbf{k}_f/k_ik_f = -\cos\theta$, $\mathbf{k}_i$ and $(\mathbf{k}_f)$ are the *c.m.s.* momenta of particles α and β in the initial and final state, respectively, $\mathbf{k}_{f1} = (m_\alpha/m_{\alpha\gamma})\,\mathbf{k}_f$, $\varkappa_{\alpha\gamma}^2 = 2\mu_{\alpha\gamma},\epsilon_{\alpha\gamma}$ is the binding energy of the bound state $(\alpha\gamma)$, and $m_{\alpha\gamma} = m_\alpha + m_\gamma$. On the basis of the diagram in Fig. 7a, it is possible to construct an infinite series of diagrams that take into account all possible successive Coulomb rescatterings of the three particles α, β, and γ in the intermediate state (diagrams b, c, d, e,... in Fig. 7). In accordance with Theorem 1, all the diagrams of this series have a singularity at $z = \zeta$. If we also take into account the Coulomb interaction of the particles in the initial and final states, we obtain for the reaction amplitude $\tilde{M}$ the expression[10]

$$\tilde{M} = \langle\Psi_{\mathbf{k}_f}^{(C)(-)}\varphi_\beta|V_\beta^N g_C V_\alpha^N|\varphi_\alpha\Psi_{\mathbf{k}_i}^{(C)(+)}\rangle. \tag{54}$$

Here, $\Psi_{\mathbf{k}_i}^{(C)(+)}$ and $\Psi_{\mathbf{k}_f}^{(C)(-)}$ are the two-particle Coulomb scattering wave functions in the initial and final states, respectively, $g_C = (E - T - V_C + i0)^{-1}$ is the three-particle Coulomb Green's function, V_α^C and V_α^N are the Coulomb and nuclear interaction potentials of particles β and γ of pair α, respectively, E (T) is the total energy (the total kinetic-energy operator) of the three-particle system, and φ_α is the wave function of the bound state of pair α. The leading singular (at $z = \zeta$) term of the amplitude $\tilde{M}$ is equal to the leading singular term $M^{(s)}$ of the exact (in the model of three charged particles) reaction amplitude M. If in (54) we replace $\Psi_{\mathbf{k}_{i,f}}^{(C)(+)}$ by the plane waves $|\mathbf{k}_{i,f}\rangle$, we obtain the amplitude B, which determines the reaction mechanism and is the sum of the infinite series of diagrams in Fig. 7.

Note that the expression (54) can be regarded as the correct generalization of the below-barrier DWBA for charged-particle transfer reactions taking into account the three-particle Coulomb dynamics of the process. If in (54) $\Psi_{\mathbf{k}_{i,f}}^{(C)(\pm)}$ is replaced by Coulomb–nuclear distorted waves, we obtain the analogous generalization of the DWBA to the case of above-barrier transfer reactions. Since $\tilde{M}$ has the correct behavior as $z\to\zeta$, where ζ is the nearest singularity, it follows from the asymptotic theorem that the contribution of the peripheral (large) partial waves is correctly taken into account in $\tilde{M}$ (in the case of below-barrier reactions, one can also speak of correct allowance for the contribution of the exterior region). Expanding g_C in a series in $\Delta V_{\alpha,\beta}^C$, where

$$\Delta V_\beta^C = V_\alpha^C + V_\gamma^C - U_\beta^C; \quad \Delta V_\alpha^C = V_\beta^C + V_\gamma^C - U_\alpha^C;$$

and U_α^C and U_β^C are the Coulomb interaction potentials of particles α and β and the center of mass of the pair α and β, respectively, we obtain

$$\tilde{M} = \langle\Psi_{\mathbf{k}_f}^{(C)(-)}\varphi_\beta|V_\alpha^N + \Delta V_\beta^C|\varphi_\alpha\Psi_{\mathbf{k}_i}^{(C)(+)}\rangle + \langle\Psi_{\mathbf{k}_f}^{(C)(-)}\varphi_\beta|\Delta V_\beta^C g_C\Delta V_\alpha^C|\varphi_\alpha\Psi_{\mathbf{k}_i}^{(C)(+)}\rangle,$$

where the first term is the amplitude of the ordinary below-barrier DWBA. It is clear that in contrast to the usual DWBA, $\tilde{M}$ takes into account all the terms of the perturbation series in $\Delta V_{\alpha,\beta}^C$.

It should be noted that $\tilde{M}$ contains not only the nearest singularity ζ with respect to z but also more distant singularities with respect to z, and therefore to find the part $\tilde{M}^{(s)}$ of the amplitude $\tilde{M}$ which is singular at $z = \zeta$ it is necessary to separate these more distant singularities. We do this separately for transfer reactions involving the neutron an charged particles.

Behavior of the amplitude of the neutron-transfer reaction near the singularity $z = \zeta$

We shall find in analytic form the leading singular term $\tilde{M}^{(s)}$ of the amplitude $\tilde{M}$ at $z = \zeta$; this determines the behavior of $\tilde{M}$ and, therefore, the exact (in the three-body model) amplitude M as $z\to\zeta$.

In the case of transfer of a neutron, $V_\alpha^C = V_\beta^C = 0$ $(\gamma = n)$ and $g_C = (E - T - V_\gamma^C + i0)^{-1}$. We rewrite (54) in the momentum representation:

$$\tilde{M}(\mathbf{k}_f, \mathbf{k}_i) = \int \frac{d\mathbf{k}'}{(2\pi)^3}\,\frac{d\mathbf{k}}{(2\pi)^3}\,\Psi_{\mathbf{k}_f}^{(C)(+)}(\mathbf{k}')\,B(\mathbf{k}', \mathbf{k})\,\Psi_{\mathbf{k}_i}^{(C)(+)}(\mathbf{k}), \tag{55}$$

where

$$B(\mathbf{k}', \mathbf{k}) = \langle\mathbf{k}', \varphi_\beta|V_\beta^N g_C V_\alpha^N|\varphi_\alpha, \mathbf{k}\rangle. \tag{56}$$

Using the relation

$$g_C = g_0 + g_0 t_\gamma^C g_0,$$

where $g_0 = (E - T + i0)^{-1}$ is the three-particle free Green's function, and

$$t_\gamma^C = V_\gamma^C + V_\gamma^C g_C V_\gamma^C$$

is the operator of Coulomb scattering of particles α and β in the three-particle space, we can express the amplitude $B(\mathbf{k}',\mathbf{k})$ as the sum of the pole diagram (a) and the triangle diagram (b) of Fig. 7 off the energy shell ($k \neq k_i$, $k' \neq k_f$). There is a singularity of the pole diagram with respect to the variable $z' = \hat{\mathbf{k}}\cdot\hat{\mathbf{k}}'/kk'$ at

$$\zeta(k', k) = (k^2 + k_1'^2 + \tilde{\varkappa}_{\alpha\gamma}^2(k'))/2kk_1' \equiv (k_1^2 + k'^2 + \tilde{\varkappa}_{\beta\gamma}^2(k))/2k_1k'; \tag{57}$$

$$k_1 = (m_\beta/m_{\beta\gamma})\,k, \quad k_1' = (m_\alpha/m_{\alpha\gamma})\,k';$$

$$\tilde{\varkappa}_{\alpha\gamma}^2(k') = \varkappa_{\alpha\gamma}^2 + (\mu_{\alpha\gamma}/\mu_f)(k'^2 - k_f^2);$$

$$\tilde{\varkappa}_{\beta\gamma}^2(k) = \varkappa_{\beta\gamma}^2 + (\mu_{\beta\gamma}/\mu_i)(k^2 - k_i^2), \tag{58}$$

$\mu_i = m_\alpha m_{\beta\gamma}/m$, $\mu_f = m_\beta m_{\alpha\gamma}/m$, $m = m_\alpha + m_\beta + m_\gamma$.

On the energy shell, $\zeta(k_f,k_i)\equiv\zeta$ [see (53)] is the singularity near which we seek the behavior of the amplitude $\tilde{M}$. The triangle diagram (b) of Fig. 7 can be obtained from the pole diagram (a) by taking into account the Coulomb scattering of particles α and β. This scattering is described by the off-shell Coulomb scattering amplitude, and therefore by Theorems 1 and 2 the triangle diagram has, like the diagram of Fig. 7a, a pole at $z = \zeta$. Besides this singularity, the triangle diagram has an intrinsic triangle singularity ζ_Δ.[52] Therefore, the amplitude $B(\mathbf{k}',\mathbf{k})$ can be written in the form

[10]The expression (54) can be obtained directly from the expression for the exact reaction amplitude by means of the Faddeev equation for the Alt–Grassberger–Sandhas transition operators.[51] It is shown thereby that simultaneous allowance for the Coulomb interaction in the initial and final states and in the intermediate state does not result in its being taken into account twice.

$$B(\mathbf{k}', \mathbf{k}) = B^{(s)}(\mathbf{k}', \mathbf{k}) + \Delta B(\mathbf{k}', \mathbf{k}), \quad (59)$$

where ΔB is the contribution from the intrinsic triangle and other nonpole singularities, and

$$B^{(s)}(\mathbf{k}', \mathbf{k}) = \Delta(k', k) B_0(\mathbf{k}', \mathbf{k}) \quad (60)$$

is the term of $B(\mathbf{k}',\mathbf{k})$ which is singular at $z' = \zeta(k',k)$, and $B_0(\mathbf{k}',\mathbf{k})$ is the amplitude of the pole diagram, given by Eq. (10) of Ref. 37, in which it is necessary to make the substitutions $\zeta \to \zeta(k',k)$, $k_i \to k$, and $k_f \to k'$; $\Delta(k',k)$ has the form[53]

$$\Delta(k', k) = \left(\frac{\sqrt{m_{\beta\gamma}m_{\alpha}r_i} + \sqrt{m_{\alpha\gamma}m_{\beta}r_f} + i\sqrt{m_{\gamma}m_{\alpha\beta}\tilde{E}}}{\sqrt{m_{\beta\gamma}m_{\alpha}r_i} + \sqrt{m_{\alpha\gamma}m_{\beta}r_f} - i\sqrt{m_{\gamma}m_{\alpha\beta}\tilde{E}}}\right)^{i\eta_{\alpha\beta}}, \quad (61)$$

$$r_i = k^2/2\mu_i - E - i0; \quad r_f = k'^2/2\mu_f - E - i0, \quad (62a)$$

$$\tilde{E} = E_{\alpha\beta} + \frac{m_{\gamma}}{m_{\alpha\beta}}\left(\frac{k'^2 - k_f^2}{2m_{\beta}} + \frac{k^2 - k_i^2}{2m_{\alpha}}\right), \quad (62b)$$

$$E_{\alpha\beta} = \frac{m_{\gamma}}{m_{\alpha\beta}}E + \frac{m_{\alpha\gamma}}{m_{\alpha\beta}}\varepsilon_{\alpha\gamma} + \frac{m_{\beta\gamma}}{m_{\alpha\beta}}\varepsilon_{\beta\gamma}, \quad (63)$$

$$\eta_{\alpha\beta} = Z_{\alpha}Z_{\beta}e^2\sqrt{\mu_{\alpha\beta}/2\tilde{E}}, \quad (64)$$

$$E = E_i - \varepsilon_{\beta\gamma}.$$

It follows from (60) that allowance for the triangle diagram with a four-leg Coulomb vertex leads to a renormalization of the pole singularity (Theorem 2) by the factor $\Delta(k',k)$.

Substituting (59) in (55), we obtain an expression for the term of the amplitude $\tilde{M}$, and, therefore, of M, which is singular at $z = \zeta$ in the case of the neutron-transfer reaction:

$$M^{(s)}(\mathbf{k}_f, \mathbf{k}_i) = \int \frac{d\mathbf{k}'}{(2\pi)^3}\frac{d\mathbf{k}}{(2\pi)^3}\Psi^{(C)(+)}_{\mathbf{k}_f}(\mathbf{k}') \Delta(k', k) B_0(\mathbf{k}', \mathbf{k}) \Psi^{(C)(+)}_{\mathbf{k}_i}(\mathbf{k}). \quad (65)$$

To find the behavior of $M^{(s)}$ as $z \to \zeta$, it is sufficient to expand it in a series in partial waves, find the behavior of the partial amplitudes $M_l^{(s)}(E_i)$ as $l \to \infty$, and then recover the behavior of $M^{(s)}(\mathbf{k}_f,\mathbf{k}_i)$ as $z \to \zeta$. An expression for $M_l^{(s)}(E_i)$ as $l \to \infty$ can be obtained by calculating the integral over k' and k by the method of steepest descent. The asymptotic expression for $\Psi^{(C)}_{\mathbf{k}_i,l}(k)$ is given by Eq. (47):

$$B_{0l}(k', k) \approx -G_{\beta}G_{\alpha}\frac{m_{\gamma}}{k'k}Q_l(\zeta(k', k)),$$

where Q_l is a Lengendre function of the second kind, and G_{α} and G_{β} are the vertex functions for the decays $(\beta\gamma) \to \beta + \gamma$ and $(\alpha\gamma) \to \alpha + \gamma$, respectively.[2] As a result, we obtain

$$M_l(E_i) \approx M_{ll}^{(s)}(E_i) \approx \exp[-(\eta_i\varphi_i + \eta_f\varphi_f)] \times \Delta(k_f, k_i) B_{0l}^{\mathrm{I}}(E_i) l^{i(\eta_i+\eta_f)}, \quad l \to \infty, \quad (66)$$

$$B_{0l}(E_i) \equiv B_{0l}(k_f, k_i),$$

$$\varphi_i = \mathrm{arctg}[(k_{f1}^2 - k_i^2 + \varkappa_{\alpha\gamma}^2)/2\varkappa_{\alpha\gamma}k_i], \quad \varphi_f = \mathrm{arctg}[(k_{i1}^2 - k_f^2 + \varkappa_{\beta\gamma}^2)/2\varkappa_{\beta\gamma}k_f]. \quad (67)$$

Since it is assumed that ζ is the nearest singularity, (66) determines the $l \to \infty$ behavior of not only $\tilde{M}_l^{(s)}$ but also $\tilde{M}_l$ and, therefore, M_l. From (66), using the expressions of Ref. 50, we obtain the leading singular term $M^{(s)}$, which determines the behavior of M as $z \to \zeta$:

$$M(\mathbf{k}_f, \mathbf{k}_i) \approx M^{(s)}(\mathbf{k}_f, \mathbf{k}_i) = N(\zeta^2 - 1)^{i\eta/2}(\zeta - z)^{-i\eta} B_0(\mathbf{k}_f, \mathbf{k}_i), \quad (68)$$

$$N = \exp[-(\eta_i\varphi_i + \eta_f\varphi_f)]\Gamma(1 + i\eta)\Delta(k_f, k_i), \quad \eta = \eta_i + \eta_f. \quad (69)$$

As $z \to \zeta$,

$$B_0(\mathbf{k}_f, \mathbf{k}_i) \approx -\frac{m_{\gamma}}{k_fk_i}\frac{G_{\beta}G_{\alpha}}{\zeta - z}. \quad (70)$$

Note that the behavior of the reaction amplitude in the DWBA as $z \to \zeta$ is given by an expression of the type (68), in which N must be replaced by

$$N_{\mathrm{post}}^{\mathrm{DWBA}} = \exp -(\eta_i\varphi_i + \eta_f\tilde{\varphi}_f)\Gamma(1 + i\eta), \quad (71a)$$

$\tilde{\varphi}_f = \mathrm{arctg}[(k_i^2 - k_{f1}^2 + \varkappa_{\alpha\gamma}^2)/2\varkappa_{\alpha\gamma}k_{f1}]$ (post form)

or

$$N_{\mathrm{prior}}^{\mathrm{DWBA}} = \exp[-(\eta_i\tilde{\varphi}_i + \eta_f\varphi_f)]\Gamma(1 + i\eta), \quad (71b)$$

$\tilde{\varphi}_i = \mathrm{arctg}[(k_f^2 - k_{i1}^2 + \varkappa_{\beta\gamma}^2)/2\varkappa_{\beta\gamma}k_{i1}]$ (prior form)[54].

It can be seen from (68) that allowance for the Coulomb effects in the initial and final states transforms the pole of the original amplitude $B_0(\mathbf{k}_f,\mathbf{k}_i)$ into a branch point, and also changes the power of this singularity, whereas allowance for the Coulomb interaction in the intermediate state (of particles α and β) changes only the power of the singularity (the factor Δ).

Behavior of the charged-particle transfer reaction amplitude near the singularity $z = \zeta$

We shall find the leading singular (at $z = \zeta$) term $M^{(s)}$ of the exact (in the model of three charged particles) reaction amplitude M (52). For this, it is necessary to find the behavior of M_l as $l \to \infty$, and then recover $M^{(s)}$. To find the asymptotic behavior of M_l, we use the results of Ref. 55, in which the method of multidimensional stationary phase was used to find the asymptotic behavior at large l of the partial-wave charge-exchange reaction amplitudes for collisions of singly charged ions with atoms. The main result of Ref. 55 is that the allowance for the three-particle Coulomb effects in the charge-exchange process leads to a simple renormalization of the asymptotic behavior of the partial-wave amplitude B_{0l} of the diagram in Fig. 7a. This result is a consequence of Theorems 1 and 2. At the same time, allowance for the Coulomb interaction of the transferred particle γ with the "cores" α and β, on the one hand, and of the cores α and β with each other, on the other hand, leads to the product of the corresponding renormalization factors. But in Ref. 55 the case $Z_{\alpha} = Z_{\beta} = -Z_{\gamma} = 1$ was considered. Therefore, there was no Coulomb interaction in the initial and final states. The presence of this Coulomb interaction changes the boundary conditions, and we take this into account by introducing partial-wave Coulomb wave functions in the initial and final states, with which we convolute the off-shell partial-wave amplitude $B_l(k',k)$, which describes the reaction mechanism (in the given case, the reaction mechanism is specified by the infinite series of diagrams in Fig. 7). The second difference between our case and the one considered in Ref. 55 relates to the use there of the approximation $m_{\gamma} \ll m_{\alpha,\beta}$. This approximation affects only the form of the renormalization factor that arises when the interaction of particles α and β is taken into account. But we have already

found this factor in the case of arbitrary masses [the expression (61)]. Using the results of Ref. 55 and the expression (61), we find that in the limit $l\to\infty$

$$B_l(k', k) = D(k', k)\, B_{0l}(k', k), \tag{72}$$

where $B_{0l}(k', k)$ is the partial-wave amplitude of the diagram in Fig. 7a off the energy shell,

$$D(k', k) = \frac{\Gamma(1-\eta_\alpha-\eta_\beta)}{\Gamma(1-\eta_\alpha)\,\Gamma(1-\eta_\beta)}\,\Delta(k', k), \tag{73}$$

and η_α (respectively, η_β) is the Coulomb parameter at the vertex $(\beta\gamma)\to\beta+\gamma((\alpha\gamma)\to\alpha+\gamma)$. Then in the limit $l\to\infty$

$$M_l(E_i) \approx \int_0^\infty \frac{dk'}{2\pi^2}\, k'^2 \int_0^\infty \frac{dk}{2\pi^2}\, k^2 \Psi^{(C)}_{lk_f}(k')\, D(k', k)$$
$$B_{0l}(k', k)\, \Psi^{(C)}_{lk_i}(k)$$
$$\approx -2\mu_{\alpha\gamma}\left(\frac{m_\beta}{m_{\beta\gamma}}\right)^{2\eta_\alpha} \exp\left[-\frac{\pi}{2}(\eta+i\eta_\alpha+i\eta_\beta)\right]\eta_\alpha\eta_\beta$$
$$\times (2k_ik_{f1})^{-1-i\eta+\eta_\alpha+\eta_\beta}\,\frac{G_\beta G_\alpha}{(4\varkappa^2_{\alpha\gamma})^{\eta_\beta}(4\varkappa^2_{\beta\gamma})^{\eta_\alpha}}$$
$$\times Df\,(\zeta^2-1)^{(-i\eta+\eta_\alpha+\eta_\beta)/2}\, l^{i\eta-\eta_\alpha-\eta_\beta}\, Q_l(\zeta), \tag{74}$$

$$D \equiv D(k_f, k_i). \tag{75}$$

In the expression (74),

$$f = \int_0^1 d\alpha_1 \int_0^{1-\alpha_1} d\alpha_3\, \frac{\alpha_1^{-1-\eta_\beta}\alpha_3^{-1-\eta_\alpha}\mathscr{K}_f^{i\eta_f}\mathscr{K}_i^{i\eta_i}}{[1+\alpha_3(\nu-1)]^{1+i\eta-\eta_\alpha-\eta_\beta}}, \tag{76}$$

$$\mathscr{K}_i = a^2-(k_i+\sqrt{u})^2;\quad \mathscr{K}_f = \frac{\mu_{\alpha\gamma}}{\mu_{\beta\gamma}}\,d\,(b^2-[k_f+i\sqrt{\rho}]^2);$$
$$a^2 = [1+(\nu-1)\alpha_3]^2k_{f1}^2;\quad u = (\nu-1)^2\alpha_3(1-\alpha_3)k_{f1}^2$$
$$+(1-\alpha_3)\varkappa^2_{\alpha\gamma}+\left(\frac{m_{\beta\gamma}}{m_\beta}\right)^2\alpha_3\varkappa^2_{\beta\gamma};$$
$$b^2 = \left[\frac{1+(\nu-1)\alpha_3}{d}\right]^2 k_{i1}^2;$$
$$\rho = \frac{[1+(\nu-1)(\alpha_1+\alpha_3)]\,d-[1+(\nu-1)\alpha_3]^2}{d^2}\,k_{i1}^2$$
$$+\frac{[1-\alpha_1+(\nu-1)\alpha_3]\,\varkappa^2_{\beta\gamma}+(\mu_{\beta\gamma}/\mu_{\alpha\gamma})\,\alpha_1\varkappa^2_{\alpha\gamma}}{d};$$
$$d = 1+(\nu-1)(\alpha_3-\nu^{-1}\alpha_1);\quad \nu = \frac{m_{\alpha\gamma}m_{\beta\gamma}}{m_\alpha m_\beta}.$$

The expression (74) can be regarded as the partial-wave amplitude of the reaction in the eikonal approximation, corresponding to $l\gg 1$, with allowance for the three-particle Coulomb effects. By virtue of

$$Q_l(\zeta) \approx \sqrt{\frac{\pi}{l}}\exp(-l\ln\tau)/\sqrt{\tau^2-1},\quad l\to\infty, \tag{77}$$

where τ and ζ are related by (46), at sufficiently large l only the contribution to the partial-wave amplitudes M_l from the nearest singularity ζ survives, and therefore in the eikonal approximation it is sufficient to take into account the contribution of only this singularity. Allowance for the Coulomb effects leads to the appearance of the factor $l^{i\eta-\eta_\alpha-\eta_\beta}$ and changes the absolute magnitude of the partial-wave reaction amplitude. Using (45) and (50a), we find the leading singular term at $z=\zeta$ of the reaction amplitude M:

$$M^{(s)}(\mathbf{k}_f, \mathbf{k}_i) = \int \frac{d\mathbf{k}'}{(2\pi)^3}\,\frac{d\mathbf{k}}{(2\pi)^3}\,\Psi^{(C)(+)}_{\mathbf{k}_f}(\mathbf{k}')\, D(k', k)$$
$$\times B_0(\mathbf{k}', \mathbf{k})\,\Psi^{(C)(+)}_{\mathbf{k}_i}(\mathbf{k}) \approx$$
$$\approx -2\mu_{\alpha\gamma}\left(\frac{m_\beta}{m_{\beta\gamma}}\right)^{2\eta_\alpha}\exp\left[-\frac{\pi}{2}(\eta+i\eta_\alpha+i\eta_\beta)\right]$$
$$\times\Gamma(1+i\eta-\eta_\alpha-\eta_\beta)\,\eta_\alpha\eta_\beta\,\frac{G_\beta G_\alpha}{(4\varkappa^2_{\alpha\gamma})^{\eta_\beta}(4\varkappa^2_{\beta\gamma})^{\eta_\alpha}}$$
$$\times Df\,\frac{1}{[2k_ik_{f1}(\zeta-z)]^{1+i\eta-\eta_\alpha-\eta_\beta}}. \tag{78}$$

Thus, without solving the Faddeev equations, we have found explicitly the asymptotic behavior of the partial-wave amplitudes and the leading singular term at $z=\zeta$ of the exact (in the model of three charged particles) reaction amplitude M. The partial-wave amplitudes M_l that we have obtained can be used to calculate surface nuclear transfer reactions, in which the main contribution is made by peripheral partial waves corresponding to $l\gtrsim kR$ [$k=(k_i+k_f)/2$, and R is the channel radius]. The expression (78) can be used to determine the vertex constant by extrapolating the experimental differential cross sections to the point of the singularity $z=\zeta$.[2] Note also that when the amplitudes of reactions with charged particles are found by solving the three-particle Faddeev–Merkurjev equations[56] serious complications arise in the calculation of the partial-wave amplitudes of the reactions at large l. The expression (74) makes it possible to restrict the calculations of the partial-wave amplitudes to small l, and then fit the calculated amplitudes to the amplitudes (74).

We shall show how these results can be used to analyze transfer reactions and obtain spectroscopic information (vertex constants).

Neutron-transfer reactions

To calculate such reactions, one generally uses the DWBA. By means of the expression (66) one can test how accurately the contribution of the peripheral partial-wave amplitudes is taken into account in the DWBA. The DWBA amplitude has the singularity $z=\zeta$ corresponding to the mechanism of Fig. 7a. The explicit form of the peripheral partial-wave amplitudes in the DWBA in the post and prior forms can be readily found from (68), (71), (50a), and (45).[11] Then we obtain

$$C_1 = M_l(E_i)/M^{\mathrm{DWBA}}_{l\,\mathrm{post}}(E_i) \underset{l\gg1}{\approx} \Delta(k_f, k_i)\exp[\eta_f(\tilde{\varphi}_f-\varphi_f)], \tag{78a}$$

$$C_2 = M_l(E_i)/M^{\mathrm{DWBA}}_{l\,\mathrm{prior}}(E_i) \underset{l\gg1}{\approx} \Delta(k_f, k_i)\exp[\eta_i(\tilde{\varphi}_i-\varphi_i)], \tag{78b}$$

where $M_l(E_i)$ is given by the expression (66).

In Table IV we give the values of C_1 and C_2 calculated for different neutron-transfer reactions $A(x,y)B$. In the calculation of the amplitudes $M_l(E_i)$, we have taken into account the contributions of the pole (a) and triangle (b) diagrams of Fig. 7 ($y=\beta$, $A=\alpha$, $n=\gamma$, $x=y+n$, $B=A+n$).

[11] The asymptotic behavior of the DWBA partial-wave amplitudes for $l\gg\eta_{i,f},\eta_{i,f}<1$, and $\sqrt{l^2+\eta^2/4}\gg1$ were found for the first time in Refs. 57 and 58.

TABLE IV. Ratio of the peripheral partial-wave amplitudes in the three-body model (M_l) and in the DWBA (M_l^{DWBA}) for neutron transfer reactions.

Reaction	E_i, MeV	c_1	c_2
^{27}Al $(d, p)^{28}$Al	10 30	1 1	1.28 1.24
^{12}C, ^{14}N, ^{13}N)^{13}C	70	1.09	1.09
^{208}Pb(^{16}O, ^{17}O)^{207}Pb	90 150	3.2 3.05	1.1 1.1

It can be seen from this table that in the case $x < A$ one must use the post form, and for $x > A$ the prior form, the difference between $M_l^{\mathrm{DWBA}}(E_i)$ and $M_l(E_i)$ for light and medium nuclei not exceeding 10% when $l \gg 1$.

Determination of the vertex constant for neutron separation from nuclei

Vertex Constant for $d \to p + n$. Calculations using realistic potentials give $G_d^2 = 0.43$ F.[2] The phenomenological value of G_d^2 can be obtained by extrapolating the experimental differential cross sections of elastic exchange $p + d$ scattering to the point of the exchange singularity $z = \zeta$ [the expression (53)]—the singularity of the diagram in Fig. 7a. For the analysis of this process, the Coulomb effects are important, and without allowance for them it is not possible to obtain the correct value of G_d^2.[59] At the same time, analysis of $n + d$ scattering, in which there are no Coulomb effects, followed by the extrapolation procedure gives values of G_d^2 in agreement withe the theoretical value of Ref. 59. In Ref. 60, the squares of the vertex constant G_d^2 were obtained by extrapolating by means of Eqs. (68) and (69) the experimental differential pd cross sections to the point of the singularity $z = \zeta$. The analysis used experimental data at 14 energies of the incident protons in the interval $3 \leqslant E_p \leqslant 46.3$ MeV. The mean value $G_d^2 = 0.427 \pm 0.003$ F obtained with allowance for the Coulomb effects is in excellent agreement with the theoretical value.

Vertex Constant for the Decay $t \to d + n$. A similar analysis of the reaction $d\,(d,p)t$ at 19 energies of the incident deuterons in the interval $4.0 \leqslant E_p \leqslant 83$ MeV gives $G_t^2 = 1.34 \pm 0.02$ F.[61] Other estimates for this vertex constant are given in the review of Ref. 2.

Vertex Constant for the Decay $^{13}\mathrm{C} \to {}^{12}\mathrm{C} + n$. Extrapolation of the experimental differential cross section of the reaction $^{12}\mathrm{C}(d,p)^{13}\mathrm{C}$(g.s.) at $E_d = 12$ MeV to the point $z = \zeta$ gives $G^2_{^{13}\mathrm{C}} = 0.4$ F,[62] in agreement with the estimates of the vertex constant obtained by other methods (see Ref. 62 and references given there).

Charged-particle transfer reactions

In this case, the peripheral partial-wave amplitudes in the DWBA can differ appreciably from the $M_l(E_i)$, and this makes it necessary to take into account three-particle Coulomb effects in the calculation of the amplitudes of charged-particle transfer reactions.

Determination of the vertex constants for separation of charged particles from nuclei

To determine the vertex constants corresponding to the disintegration of nuclei into two charged fragments, use was made of the peripheral model,[37] in whcih the expression (74) was used to calculate the peripheral partial waves.

The $^6\mathrm{Li}(d,{}^6\mathrm{Li})^2\mathrm{H}$ Reaction. In the experimental angular distributions of $d\,{}^6$Li elastic scattering at energies $E_d = 8$–14.7 MeV of the incident deuterons in the laboratory system,[63,64] there is a sharp rise at large angles (Fig. 8). It can be explained naturally by assuming that at large θ the main contribution to the scattering cross section is made by the singularity with respect to z of the α-particle exchange mechanism (the diagram in Fig. 7a, in which $\alpha = \beta = d$, $\gamma = {}^4$He), this singularity being much closer to the boundary $z = 1$ of the physical region than the singularities corresponding to the other simplest mechanism described by loop (transfer of a pair of particles: pt, n^3He, dd) or triangle diagrams.[65] However, all the diagrams of Fig. 7 corresponding to allowance for Coulomb rescatterings of two deuterons and an α particle in the intermediate state have singularities at the same place as the diagram in Fig. 7a, and they must be

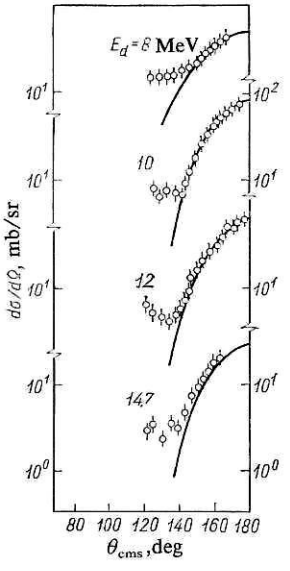

FIG. 8. Differential cross section of $d\,{}^6$Li elastic scattering at large angles. The continuous curves represent our calculation in the peripheral model with allowance for Coulomb effects.

TABLE V. Nuclear vertex constants for the decay $^6\text{Li} \to \alpha + d$.

E_d, MeV	$G^2_{\alpha d}$, F
8.0	0.16 (0.48)
10.0	0.34 (0.97)
12.0	0.31 (0.86)
14.7	0.24 (0.63)
Average	0.26 (0.74)

taken into account in the calculation. The calculated differential cross sections are given in Fig. 8. The contribution of the D state to he $^6\text{Li} \rightleftarrows \alpha + d$ vertices was not taken into account. It can be seen that the calculated angular distributions describe well the experimental distributions at large angles, and Coulomb rescattering in the initial and final states and the three-particle Coulomb effects have almost no influence on the shape of the angular distributions in this region.

The squares of the vertex constants $G^2_{\alpha d}$ for the $^6\text{Li} \to \alpha + d$ decay found by comparing the calculated and experimental differential cross sections are given in Table V, in which the quantities in brackets are the values of $G^2_{\alpha d}$ obtained using the DWBA peripheral partial-wave amplitudes, in which three-particle Coulomb effects are not taken into account. Allowance for the latter in the peripheral partial-wave amplitudes increases the theoretical cross section by about eight times, and this reduces the values of $G^2_{\alpha d}$ that are extracted by about 2.8 times. We note that the Coulomb interaction in the three-leg $^6\text{Li} \rightleftarrows \alpha + d$ vertices in the diagram in Fig. 7a increases the extracted values of $G^2_{\alpha d}$ by about two times[2] (this interaction is also taken into account in the DWBA), whereas simultaneous allowance for the Coulomb interaction in the three-leg vertices and the three-particle Coulomb effects decreases the determined value of $G^2_{\alpha d}$ in the case considered. This example shows how important it is to take into account all the Coulomb effects at once. We note that the estimates of $G^2_{\alpha d}$ in the literature obtained by different methods differ strongly from each other.[2] In Ref. 66, a variational stochastic method was used to find the wave function of the ^{6}Li nucleus in the αpn model. The wave functions with correct asymptotic behavior obtained by this method gives $G^2_{\alpha d} = 0.46$ F.

The $^7\text{Li}(d,^6\text{Li})\,^2\text{H}$ *Reaction.* The angular distribution in this reaction at the energy $E_d = 12$ MeV has a peak at $\theta = 180°$.[67] The singularity nearest the point $z = 1$ is the singularity of the diagram of Fig. 7a describing α-particle transfer ($\alpha = d, \beta = {}^3\text{H}$, and $\gamma = {}^4\text{He}$). The differential cross section was calculated in the framework of the peripheral model (Fig. 9). The influence of the Coulomb effects is qualitatively the same as in the previous reaction. In particular, they hardly affect the shape of the calculated angular distribution, which was fitted to the experimental one at large angles ($\theta \gtrsim 150°$), where one must expect a dominant contribution of the α-particle pickup mechanism (the diagram of Fig. 7a). Since the differential cross section in the peripheral model is

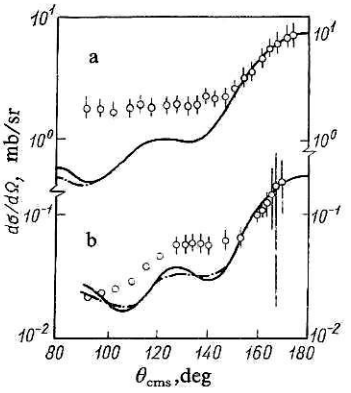

FIG. 9. Differential cross sections of the following reactions: a) $^7\text{Li}(d, ^6\text{Li})^3\text{H}$ at $E_d = 12$ MeV (Ref. 67); b) $^7\text{Li}(p,\alpha)^4\text{He}$ at $E_p = 45.2$ MeV.[68] The curves are the results of calculations in accordance with the peripheral model (continuous curve with allowance for the Coulomb effects, broken curve without it).

proportional to $G^2_{\alpha t}\, G^2_{\alpha d}$, where $G^2_{\alpha t}$ is the square of the vertex constant for the $^7\text{Li} \to \alpha + t$ decay, it is possible to determine $G^2_{\alpha t}\, G^2_{\alpha d}$ by comparing the calculated and experimental differential cross sections at large angles. $G^2_{\alpha d} = 0.26$ F, the values $G^2_{\alpha t} = 0.33$ F is obtained.

The $^7\text{Li}(\text{p},\alpha)^4\text{He}$ *Reaction.* The peripheral model was used to calculate the differential cross section of this reaction at energy 45.2 MeV of the incident protons (Fig. 9) under the assumption that the peak in the experimental angular distribution at large angles[68] is due to the singularity with respect to z of the triton-transfer mechanism (the diagram of Fig. 7a with $\alpha = p$, $\beta = {}^4\text{He}$, and $\gamma = {}^3\text{H}$). With allowance for the Coulomb effects, the value $G^2_{\alpha t} = 0.28$ F was found. For this, we used for the $\alpha \to t + p$ decay the square of the vertex constant $G^2_{tp} = 12.4$ F, this being the mean of the G^2_{tp} and $G^2_{\tau n}$ ($\tau = {}^3\text{He}$) found in Refs. 69–71 by analysis of experimental data using a forward dispersion relation. In this reaction, the influence of the Coulomb effects is least because of the large value of E_p and the large binding energy in the three-leg vertex $t + p \to \alpha$. It can be seen that the values of $G^2_{\alpha t}$ obtained by analyzing the two different reactions are nearly equal.

Thus, we have analyzed the three reactions with the lightest nuclei. The Coulomb redistribution in the initial and final states has the greatest effect on the shape of the angular distributions, but it is appreciable only at large η_i and η_f. In the cases which we have considered, $\eta_{i,f} < 0.3$, and therefore the effect of the Coulomb interaction on the shape of the angular distributions in the reactions considered is slight. The situation is different in heavy-ion reactions, for which $\eta_{i,f} \gg 1$.

Angular distributions in transfer reactions initiated by heavy ions

Reactions in which a nucleon or a group of nucleons is transferred at energies around the Coulomb barrier belong to the class of reactions in which the Coulomb interaction plays a decisive part in the formation of the angular distributions. The angular distributions in such reactions have, as a

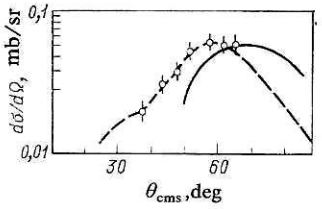

FIG. 10. Differential cross sections of the reaction ^{40}Ca(^{16}O,^{15}N)^{41}Sc(g.s.) at energy 48 MeV of the incident ^{16}O ions, taken from Ref. 72. The curves represent DWBA calculations (the continuous curve with the standard values of the parameters of the optical potentials, and the broken curve with a modified optical potential in the exit channel).

rule, a bell-shaped form with a peak at $\theta \approx \theta_0$, where θ_0 is the scattering angle of nuclei moving along Rutherford trajectories corresponding to a "glancing" collision. A typical bell-shaped experimental angular distribution is shown in Fig. 10. The reason for the occurrence of the peak in the angular distribution is the competition between the Coulomb repulsion and the nuclear attraction. At large impact parameters ρ corresponding to small θ, the probability of transfer of a particle from nucleus to nucelus is small because of the weak overlapping of the wave functions of the bound states of the transferred particle in the initial and final nuclei. At small ρ ($\rho < R_1 + R_2$, where $R_{1,2}$ are the interaction ranges of the nuclei), the probability of quasielastic (direct) transfer[12)] of a particle is small because of the strong absorption that arises as a result of the competition between the large number of open channels. The maximal transfer probability occurs for nearly grazing trajectories of the nuclei ($\rho \approx \rho_0, \rho_0 = R_1 + R_2$). Therefore, the peak that corresponds to them in the angular distribution is often called the grazing peak. Because of the strong Coulomb repulsion, θ_0 is several tens of degrees. With decreasing energy, the grazing peaks are shifted to larger angles, and the value of the cross section at the peak decreases. With increasing energy, these peaks are shifted to smaller angles, and the angular distribution gradually goes over into the usual diffraction distribution. An elegant explanation of the mechanism of occurrence of the grazing peak in the angular distribution at $\theta \approx \theta_0$ was given by Strutinskiĭ,[74] who obtained the following approximate condition for the occurrence of the peak:

$$\theta_0/\lambda > 2, \tag{79}$$

where θ_0 can be estimated by means of the relation

$$\theta_0 \approx 2\operatorname{arctg} \eta/l_0. \tag{80}$$

Here, $\eta = (\eta_i + \eta_f)/2$, $l_0 \approx k_{\text{eff}}\rho_0, k_{\text{eff}} = \sqrt{2\mu(E_i - V(\rho_0)}$, E_i) is the relative kinetic energy of the colliding particles, and $V(\rho_0)$ is the interaction potential of the nuclei at the point at which they touch. The parameter λ is related to the asymptotic behavior of the partial-wave reaction amplitude in the plane-wave approximation when $l \gg 1$ by

$$B_l(E_i) \approx \exp(-\lambda l). \tag{81}$$

Using the expression (45), it is possible to relate λ to the characteristics of the diagram that describes the transfer reaction mechanism. For $(l - l_0)/l_0 \ll 1$ and $l \geqslant l_0 \gg 1$,

$$\lambda = \ln \tau + \left(\chi + \frac{3}{2}\right)\Big/ l_0, \tag{82}$$

where τ and χ are given by the expressions (46). Thus, the relations (79) and (82) make it possible to estimate the mechanisms for which a grazing peak is possible. We emphasize, however, that the condition (97) must be regarded as approximate, since its derivation used a number of strong simplifying assumptions; in particular, the nuclear phase shifts for $l > l_0$ were not taken into account, and the Coulomb phase shifts were expanded in a series around the point $l = l_0$ and only the first two terms in the expansion were retained. The calculations also show that the nature of the angular distributions in the region of the grazing peak depends on the parameters of the optical potentials in the entrance and exit channels of the reaction. A detailed study, in the framework of the diffraction model, of the reasons for the occurrence of the grazing peak in neutron transfer reactions induced by heavy ions was made in Ref. 58.

Besides the problem of the occurrence of the grazing peak, it is also of interest to find an exact description of its position as a function of the reaction characteristics (energy of the incident ion, Q of the reaction). Calculations of the angular distributions of neutron-transfer reactions in the framework of the DWBA agree, as a rule, with the experimental data.[75] However, in the case of proton transfer at large negative Q of the reaction, the experimental grazing peaks are to the left of the peaks predicted by the DWBA, and with increasing $|Q|$ and decreasing E_i the difference increases.[72,75] A still larger difference is observed even at small $|Q|$ in the case of α-particle transfer.[76] The shift of the experimental peaks to the left indicates that in the case of transfer of a charged particle the relative contribution of the peripheral partial-wave amplitudes is in fact greater than in the DWBA. The increase in the relative contribution of the peripheral partial-wave amplitudes leads to an increase in the transfer probability at large ρ, i.e., to a displacement of the grazing peak to smaller angles. Since a difference between the theoretical and experimental angular distributions appears only in the case of the transfer of charged particles at energies near the Coulomb barrier, it is clear that the reason for the discrepancy is the inaccurate allowance for the Coulomb effects in the DWBA. Figure 10 shows the angular distributions of the reaction ^{40}Ca(^{16}O,^{15}N)^{41}Sc(g.s.) at $E_i = 34.3$ MeV given by the DWBA. To describe the experimental angular distributions, the parameters of the optical potentials are usually varied artificially, for example, the diffuseness of the potential in the exit channel is increased.[72] However, when the potential is modified in this way, it does not describe the elastic scattering. The observed discrepancy between theory and experiment can be explained by taking into account the three-particle Coulomb effects. When they are taken into account, the relative contribution of the peripheral amplitudes is increased.

CONCLUSIONS

Our study in this paper confirms the important part played by Coulomb effects in the various approaches to the

[12)] We do not consider here deep inelastic reactions between heavy nuclei, when a peak must also appear in the angular distribution at $\theta \approx \theta_0$.[73]

theory of nuclear reactions, particularly in the case of processes at low energies or with the participation of weakly bound systems. At the same time, it follows from the above that correct allowance for the Coulomb interaction makes it possible to obtain a reasonable description of the experimental data on nuclear reactions with charged particles and to obtain for them valuable spectroscopic information.

The Coulomb interaction significantly changes the analytic properties of the scattering amplitudes; a striking illustration of this change is the nontrivial fact, discussed in Sec. 9, of the appearance of pole singularities corresponding to the mechanism of single-particle transfer in nonpole diagrams (triangle, etc.).

In this review, of course, we have not attempted to discuss all the questions associated with the manifestation of Coulomb effects in nuclear processes. In particular, we have not considered the problem of taking into account the Coulomb interaction in the solution of the Faddeev equations for a system of three charged particles. This important problem, the practical solution of which cannot yet be regarded as completed, has been the subject of quite a considerable number of studies (see, for example, Refs. 51, 56, and 77–81). In this connection, we note that the results obtained in Sec. 9 can be used to simplify the Alt–Grassberger–Sandhas equations with three charged particles[79] by the replacement of the nondiagonal potentials of the transitions in these equations, which contain three-particle Coulomb Green's functions, by their leading singular terms. The approximate equations then obtained can be used to calculate the amplitudes of nuclear reactions in the model of three charged particles. But all this is a special subject in its own right.

[1]A. G. Baryshnikov, L. D. Blokhintsev, A. N. Safronov, and V. V. Turovtsev, Nucl. Phys. **A224**, 61 (1974).
[2]L. D. Blokhintsev, I. Borbely, and É. I. Dolinskiĭ, Fiz. Elem. Chastits At. Yadra **8**, 1189 (1977) [Sov. J. Part. Nucl. **8**, 485 (1977)].
[3]A. M. Badalyan and Yu. A. Simonov, Fiz. Elem. Chastits At. Yadra **6**, 299 (1975) [Sov. J. Part. Nucl. **6**, 119 (1975)].
[4]D. Y. Wong and H. P. Noyes, Phys. Rev. **126**, 1866 (1962).
[5]Yu. L. Mentkovskiĭ, Chastitsa v yaderno-kulonovskom pole (Particle in a Coulomb–Nuclear Field), Énergoatomizdat, Moscow (1982).
[6]J. Hamilton *et al.*, Nucl. Phys. **60**, 443 (1973).
[7]A. I. Baz', Ya. B. Zel'dovich, and A. M. Perelomov, Rasseyanie, reaktsii i raspady v nerelyativistskoĭ kvantovoĭ mekhanike, 2nd Ed., Nauka, Moscow (1971); English translation of 1st Ed.: Scattering, Reactions and Decay in Nonrelativistic Quantum Mechanics, Jerusalem (1969).
[8]L. D. Blokhintsev and A. N. Safronov, Izv. Akad. Nauk SSSR **47**, 2168 (1983).
[9]V. de Alfaro and T. Regge, Potential Scattering, North-Holland, Amsterdam (1965) (Russian translation published by Mir, Moscow (1966)).
[10]A. N. Safronov, Izv. Akad. Nauk Kaz. SSR, Ser. Fiz.-Mat. No. 2, 31 (1982).
[11]H. Van Haeringen, J. Math. Phys. **17**, 995 (1976); **18**, 927 (1977); **20**, 2520 (1979).
[12]M. L. Goldberger and K. M. Watson, Collision Theory, Wiley, New York (1964) (Russian translation published by Mir, Moscow (1967)).
[13]C. Lovelace, Phys. Rev. **135**, B1225 (1964).
[14]L. D. Blokhintsev and A. N. Safronov, Izv. Akad. Nauk SSSR, Ser. Fiz. **46**, 925 (1982).
[15]J. Humblet, Phys. Lett. **B32**, 553 (1970).
[16]F. Nichitiu, Fazovyĭ analiz v fizike yadernykh vzaimodeĭstviĭ (Phase-Shift Analysis in the Physics of Nuclear Interactions; Russian translation from the Rumanian), Mir, Moscow (1983).
[17]J. Fröhlich *et al.*, J. Phys. G**6**, 841 (1980); Phys. Lett. **B82**, 173 (1979); **B92**, 8 (1980); Z. Phys. A **302**, 89 (1981).
[18]R. Dubois *et al.*, Nucl. Phys. **A377**, 529 (1982).
[19]L. D. Blokhintsev and A. N. Safronov, Czech. J. Phys. **B32**, 340 (1982).
[20]L. D. Blokhintsev and A. N. Safronov, Problemy yadernoĭ fiziki i kosmicheskikh lucheĭ (Problems of Nuclear Physics and Cosmic Rays), No. 11 (1979), p. 7.
[21]A. N. Safronov, in: Tezisy dokladov XXXII soveshchaniya po yadernoĭ spektroskopii i strukture atomnogo yadra (Abstracts of Papers at the 32nd Symposium on Nuclear Spectroscopy and Nuclear Structure), Nauka, Leningrad (1982), p. 405.
[22]A. N. Safronov, in: Tezisy dokladov XXXIII soveshchaniya po yadernoĭ spektroskopii i strukture atomnogo yadra (Abstracts of Papers at the 33rd Symposium on Nuclear Spectroscopy and Nuclear Structure), Nauka, Leningrad (1983), p. 456.
[23]A. N. Safronov, Pis'ma Zh. Eksp. Teor. Fiz. **37**, 608 (1983) [JETP Lett. **37**, 727 (1983)].
[24]J. M. Greben, Phys. Lett. **B115**, 363 (1982).
[25]D. N. Hardy *et al.*, Nucl. Phys. **A195**, 250 (1972).
[26]D. H. McSherry and S. D. Baker, Phys. Rev. C **1**, 888 (1970).
[27]W. Dilg *et al.*, Phys. Lett. **B36**, 208 (1971).
[28]J. Arvieux, Nucl. Phys. **A221**, 253 (1974).
[29]M. U. Ahmed and P. E. Shanley, Phys. Rev. Lett. **36**, 25 (1976).
[29a]D. R. Lehman and B. F. Gibson, Phys. Rev. C **16**, 1275 (1977).
[30]J. S. Ball *et al.*, Phys. Rev. Lett. **28**, 1143 (1972); Phys. Rev. D **11**, 1171 (1975).
[31]R. A. Arndt *et al.*, Phys. Rev. C **3**, 2100 (1971).
[32]R. A. Arndt *et al.*, Nucl. Phys. **A209**, 429 (1973).
[33]R. A. Arndt *et al.*, Nucl. Phys. **A209**, 447 (1973).
[34]F. Ajsenberg-Selove, Nucl. Phys. **A227**, 1 (1974); **A320**, 1 (1979).
[35]A. N. Safronov, in: Tezisy dokladov XXXI soveshchaniya po yadernoĭ spektroskopii i strukture atomnogo yadra (Abstracts of Papers at the 31st Symposium on Nuclear Spectroscopy and Nuclear Structure), Nauka, Leningrad (1981), p. 467.
[36]G. Baur and L. Trautmann, Phys. Rep. **25**, 294 (1976).
[37]E. I. Dolinsky, P. O. Dzhamalov, and A. M. Mukhamedzhanov, Nucl. Phys. **A202**, 97 (1973).
[38]É. I. Dolinskiĭ *et al.*, Yad. Fiz. **29**, 71 (1979) [Sov. J. Nucl. Phys. **29**, 34 (1979)].
[39]P. O. Dzhamalov and É. I. Dolinskiĭ, Yad. Fiz. **14**, 753 (1971) [Sov. J. Nucl. Phys. **14**, 423 (1972)].
[40]Ya. B. Zel'dovich, Zh. Eksp. Teor. Fiz. **39**, 776 (1960) [Sov. Phys. JETP **12**, 542 (1961)].
[41]I. S. Gradshteĭn and I. M. Ryzhik, Tablitsy integralov, summ, ryadov i proizvedeniĭ, Fizmatgiz, Moscow (1962); English translation: Table of Integrals, Series, and Products, Academic Press, New York (1965).
[42]É. I. Dolinskiĭ and A. M. Mukhamedzhanov, Izv. Akad. Nauk SSSR, Ser. Fiz. **41**, 2055 (1977).
[43]A. M. Mukhamedzhanov, R. Yarmukhamedov, and P. O. Dzhamalov, Yad. Fiz. **37**, 1405 (1983) [Sov. J. Nucl. Phys. **37**, 838 (1983)].
[44]I. Borbeĭ *et al.*, Yad. Fiz. **26**, 516 (1977) [Sov. J. Nucl. Phys. **26**, 274 (1977)].
[45]I. S. Shapiro, Zh. Eksp. Teor. Fiz. **41**, 1616 (1961) [Sov. Phys. JETP **14**, 1148 (1962)]; Teoriya pryamykh yadernykh reaktsiĭ (Theory of Direct Nuclear Reactions), Atomizdat, Moscow (1963); Usp. Fiz. Nauk **92**, 549 (1967) [Sov. Phys. Usp. **10**, 515 (1968)].
[46]L. D. Blokhintsev and É. Truglik, Zh. Eksp. Teor. Fiz. **53**, 2176 (1967) [Sov. Phys. JETP **26**, 1229 (1968)]; L. D. Blokhintsev, A. N. Safronov, and I. A. Shvarts, Teor. Mat. Fiz. **24**, 90 (1975).
[47]É. I. Dolinskiĭ and A. M. Mukhamedzhanov, Yad. Fiz. **3**, 252 (1966) [Sov. J. Nucl. Phys. **3**, 180 (1966)].
[48]E. Guth and C. J. Mullin, Phys. Rev. **83**, 667 (1951).
[49]A. M. Perelomov and V. S. Popov, Zh. Eksp. Teor. Fiz. **50**, 179 (1966) [Sov. Phys. JETP **23**, 118 (1966)].
[50]V. S. Popov, Zh. Eksp. Teor. Fiz. **47**, 2229 (1964) [Sov. Phys. JETP **20**, 1494 (1965)].
[51]E. O. Alt, W. Sandhas, and H. Ziegelmann, Phys. Rev. C **17**, 1981 (1978).
[52]L. D. Blokhintsev, É. I. Dolinskiĭ, and V. S. Popov, Zh. Eksp. Teor. Fiz. **42**, 1636 (1962) [Sov. Phys. JETP **15**, 1136 (1962)]; Nucl. Phys. **40**, 117 (1963).
[53]E. I. Dolinsky and A. M. Mukhamedzhanov, Czech. J. Phys. **B32**, 302 (1982).
[54]F. D. Santos and P. Colby, Nucl. Phys. **A367**, 197 (1981).
[55]Yu. N. Demkov and V. N. Ostrovskiĭ, Zh. Eksp. Teor. Fiz. **69**, 1582 (1975) [Sov. Phys. JETP **42**, 806 (1975)].
[56]S. P. Merkurjev, Acta Phys. Austriaca Suppl. **33**, 65 (1981).
[57]A. V. Shebeko, Yad. Fiz. **13**, 1259 (1971) [Sov. J. Nucl. Phys. **13**, 724 (1971)].
[58]V. V. Kotlyar and A. V. Shebeko, Z. Phys. A **299**, 311 (1981).

[59]I. Borbely, J. Phys. G **5**, 937 (1979).
[60]A. M. Mukhamedzhanov *et al.*, Izv. Akad. Nauk SSSR, Ser. Fiz. **48**, 350 (1984).
[61]I. Borbely and A. M. Mukhamedzhanov, in: Tezisy dokladov XXXIV soveshchaniya po yadernoĭ spektroskopii i strukture atomnogo yadra (Abstracts of Papers at the 34th Symposium on Nuclear Spectroscopy and Nuclear Structure), Alma-Ata (1984), p. 413.
[62]S. A. Goncharov *et al.*, Yad. Fiz. **35**, 662 (1982) [Sov. J. Nucl. Phys. **35**, 383 (1982)].
[63]H. G. Bingham *et al.*, Nucl. Phys. **A173**, 265 (1971).
[64]S. Matsuki *et al.*, J. Phys. Soc. Jpn. **26**, 1344 (1969).
[65]G. V. Avakov *et al.*, Problemy yadernoĭ fiziki i kosmicheskikh lucheĭ (Problems of Nuclear Physics and Cosmic Rays), No. 7, Vishcha Shkola, Khar'kov (1977), p. 80.
[66]V. I. Kukulin, V. M. Krasnopolsky, V. T. Voronchev, and P. B. Sazonov, Nucl. Phys. **A417**, 128 (1984).
[67]A. R. Zander, K. W. Kemper, and N. R. Fletcher, Nucl. Phys. **A173**, 273 (1971).
[68]R. M. Craig *et al.*, Nucl. Phys. **A96**, 367 (1967).
[69]M. P. Locher, Nucl. Phys. **B36**, 634 (1972).
[70]G. R. Plattner *et al.*, Nucl. Phys. **A206**, 513 (1973).
[71]M. P. Locher, Nucl. Phys. **A251**, 493 (1975).
[72]H. J. Körner *et al.*, Phys. Rev. C **7**, 107 (1973).
[73]V. V. Volkov, Yadernye reaktsii glubokoneuprugikh Peredach (Nuclear Reactions of Deep Inelastic Transfers), Énergoizdat, Moscow (1982).
[74]V. M. Strutinskiĭ, Zh. Eksp. Teor. Fiz. **46**, 2078 (1964) [Sov. Phys. JETP **19**, 1401 (1964)].
[75]T. Tamura, T. Udagawa, and M. C. Mermaz, Phys. Rep. **65**, 345 (1980).
[76]G. P. A. Berg *et al.*, Phys. Rev. C **18**, 2204 (1978).
[77]A. M. Veselova, Teor. Mat. Fiz. **13**, 368 (1972); **35**, 180 (1978).
[78]V. F. Kharchenko and S. A. Shadchin, Ukr. Fiz. Zh. **23**, 1651 (1978).
[79]E. O. Alt and W. Sandhas, Phys. Rev. C **21**, 1733 (1980).
[80]S. P. Merkur'ev and S. A. Pozdneev, Yad. Fiz. **30**, 941 (1979) [Sov. J. Nucl. Phys. **30**, 489 (1979)].
[81]S. Pozdneev, J. Phys. G **8**, 1509 (1982).

Translated by
Julian B. Barbour